

ADP-01-15/T450

LTH ??

Electron-Nucleus Collisions at THERA

L. Frankfurt¹, V. Guzey², M. McDermott³, and M. Strikman⁴

¹ *School of Physics and Astronomy, Tel Aviv University, 69978 Tel Aviv, Israel*

² *Special Research Centre for the Subatomic Structure of Matter (CSSM), Adelaide University, 5005, Australia.*

³ *Division of Theoretical Physics, Dept. of Math. Sciences, University of Liverpool, Liverpool L69 3BX, England.*

⁴ *Department of Physics, Pennsylvania State University, University Park, PA 16802, USA*

(December 4, 2018)

Abstract

The nuclear option at THERA provides an ideal and unique opportunity to investigate the black body limit (BBL) of high energy Deep Inelastic Scattering of highly virtual photons off heavy nuclear targets and thereby probe QCD in a new regime. At high enough energies, whichever hadronic configuration the photon fluctuates into, the interaction at a given impact parameter with the heavy nuclear target will eventually reach its geometrical limit corresponding to the scattering from a black disk. An attractive feature of the BBL regime for a large nucleus is that the interaction is strong although the coupling constant is small. Predictions for longitudinal and transverse distributions of the leading hadrons in inclusive and diffractive channels and exclusive vector meson production are found to be strikingly different in BBL

and the leading twist approximation. In particular, the multiplicity of leading hadrons in the current fragmentation region is strongly suppressed, while the cross section of diffractive vector meson production by longitudinally polarized photons is $\propto 1/Q^2$. The x and Q^2 ranges where BBL maybe reached are calculated for the interaction of color triplet and color octet dipoles at central impact parameters. We conclude that for heavy nuclei THERA would reach deep into BBL for a wide range of Q^2 . The connection between hard diffraction and leading twist nuclear shadowing is analysed. It is demonstrated that the current leading twist analyses of the HERA diffractive data lead to similar and very large leading twist shadowing for gluons. Several processes sensitive to the amount of nuclear shadowing for gluons are discussed.

I. EXECUTIVE SUMMARY

The nuclear option at THERA provides an ideal and unique opportunity to investigate the black body limit (BBL) of high energy Deep Inelastic Scattering (DIS) of highly virtual photons off heavy nuclear targets and thereby probe Quantum Chromodynamics (QCD) in a new regime. At high enough energies, whichever hadronic configuration the photon fluctuates into, the interaction at given impact parameter with the heavy nuclear target will eventually reach its geometrical limit corresponding to the scattering from a black disk. An attractive likely feature of the approach to the BBL regime for a large nucleus is that the interaction is strong although the coupling constant is small. Predictions for many observables are qualitatively different within the BBL from those of the standard leading twist DGLAP [1] regime. The most striking predictions for inclusive observables include: (i) the nuclear structure functions behave as $F_2^A \propto \pi R_A^2 Q^2 \ln(1/4m_N R_A x)$, with a $1/x$ dependence slower than that predicted by DGLAP (this is in contrast with the nucleon case in which $F_2^N \propto Q^2 \pi R_N^2 (1 + c_N \ln^2 1/x) \ln 1/x$ whose x dependence is comparable with the DGLAP prediction, here R_A, R_N are radii of nucleus and nucleon), (ii) the ratio of nuclear

and nucleon structure functions decreases with $1/x$, $F_2^A/F_2^N \propto 1/(1 + c_N \ln^2 1/x)$. Major new features for the final states in DIS are: (i) a much softer leading hadron spectra with enhanced production of high p_t jets in inclusive and diffractive processes, (ii) the inclusive diffractive cross section reaches nearly half of the total cross section, (iii) a weakly Q^2 -dependent parameter-free cross section for exclusive vector meson electroproduction.

It is possible that the black limit will be reached for certain gluon-induced DIS processes off nucleons within THERA kinematics. However, nuclei have two very clear and useful advantages over nucleon targets. Firstly, because the target is extremely Lorentz contracted, the partons of individual nucleons are piled up on one another. This means that for a given photon-target centre of mass energy the black limit will be reached *much earlier* in nuclei. Secondly, scattering from the edge of nucleons, which remains grey even at very high energies, (and competes with the BBL contribution) is heavily suppressed for large nuclei. The purpose of the rest of this report is to expand on the details for the interested reader.

II. INTRODUCTION

The standard theoretical approach to inclusive Deep Inelastic Scattering (DIS) of a virtual-photon off a target, $\gamma^*(q) + T(p) \rightarrow X$, uses a factorization theorem [2] to prove that in the limit of large photon virtuality ($q^2 = -Q^2 \ll 0$), leading twist (LT) terms dominate in the Operator Product Expansion [3] of the relevant hadronic matrix elements. This corresponds to a factorization of short and long distance contributions and leads to an attractive physical picture of the virtual photon scattering off electrically charged “point-like” partonic constituents within the target, with its associated approximate Bjorken [4] scaling (which states that structure functions, for example, F_L and F_2 , only depend on the ratio $x = Q^2/2p \cdot q$). The application of the renormalization group to perturbative Quantum Chromodynamics (pQCD), embodied in the DGLAP [1] evolution equations, corrects this naive picture and leads to logarithmic scaling violations. These equations describe how the long-distance boundary conditions, the parton distributions of the quarks and gluons, (and

ultimately F_L and F_2) change logarithmically with Q^2 .

It is now understood that this decomposition in terms of twists should become inapplicable in pQCD at sufficiently small x (i.e. the higher twist (HT) terms, which are formally suppressed by positive integer powers of $1/Q^2$, become numerically important). However, in practice, it is very difficult to distinguish HT effects in the inclusive structure functions from uncertainties in the input parton distributions for a nucleon target, because DIS off the nucleon edge masks the importance of the HT effects. We will explain that the theoretical description of DIS off heavy nuclei is significantly simpler than that for a nucleon target. The energy and Q^2 dependence of structure functions of heavy nuclei, and specific properties of final states, can serve as clear signatures of a new regime, the black body limit (BBL) regime, where significant contributions to the dynamics of the strong interactions from all twists are expected.

For the past decade, pQCD has been used extremely successfully to describe inclusive DIS processes (see e.g. [5]). Many new phenomena specific to small- x physics have been discovered experimentally and explained by pQCD. New QCD factorization theorems for certain hard processes (such as diffractive scattering [6], exclusive vector meson production [7,8] and Deeply Virtual Compton Scattering [9]) have been proven. These factorization theorems were used to predict and describe qualitatively new small- x hard scattering phenomena. In particular, hard exclusive processes for both nucleon and nuclear targets, with properties strikingly different from those familiar from soft hadronic processes, were predicted and observed (several experimental [10] and theoretical [11–13] reviews are available in the literature). These include: (i) the complete transparency of nuclear matter in coherent pion diffraction into two jets off a nuclear target (predicted in [14] and later observed in [15]) and in exclusive photoproduction of J/ψ mesons off nuclei [16], (ii) a fast increase with increasing energy of cross sections of hard exclusive processes [17]: high Q^2 exclusive ρ , ϕ , J/ψ meson production [7,18–21] and exclusive photoproduction of J/ψ and Υ mesons [22], [23] and low- x exclusive photon production in DIS (Deeply Virtual Compton Scattering [24]), (iii) an almost universal and small slope of the t -dependence of hard exclusive processes

(predicted in [25]), (iv) a small and process/scale dependent rate of change of the slope of t -dependence of exclusive processes with energy, α' , (v) confirmation that QCD is flavour blind in hard (high Q^2) exclusive vector meson (ρ and ϕ mesons) electroproduction. These theoretical and experimental discoveries have moved the focus of investigations in QCD to new frontiers.

A seminal and extremely important experimental observation is the fast increase with $1/x$ of the proton structure function, F_2 , at small x discovered by the H1 [26] and ZEUS [27] collaborations at HERA. The implied fast increase of the proton parton densities raises several challenging questions for DIS at even higher energies:

- Will it remain sufficient to use the leading twist DGLAP evolution equation (to a given accuracy in logarithms in Q^2) or will it become necessary to resum [28–30] the large logs in energy that appear at each order in the perturbative expansion (i.e. for the regime in which $\alpha_s(Q^2) \ln(x_0/x) \sim \mathcal{O}(1)$) ?
- Does diffusion in parton transverse momenta lead to a breakdown of (collinear) factorization for leading twist pQCD, and a non-trivial mixing of perturbative and non-perturbative effects, in a kinematic regime in Q^2 which is assumed to be safe at higher x ?
- Will the increase of the parton distributions lead to an experimentally-accessible new pQCD regime, where the coupling constant is small but the interaction is strong ? If so, how can one distinguish between this new regime and the standard one in which the LT DGLAP equations are applicable ?
- Will the structure functions and cross sections of hard exclusive processes continue to increase with energy or will their growth be tamed to avoid violation of unitarity of the S -matrix (applied to the hard interactions of the hadronic fluctuations of the photon) ?

- Since the same QCD factorization theorems which lead to successful description of hard processes predict a rapid increase of HT effects with increasing energy, how important will the latter effects be for the interpretation of the small- x data ?

In the following we explain that one has a good chance to answer these questions by studying electron-nucleus collisions at THERA. We will formulate several theoretical predictions, based mostly on general properties of space-time evolution of high-energy scattering, which can serve as signals of new hard QCD phenomena.

DIS at high energies is most easily formulated in the target rest frame (this approach has become known as *the dipole picture* for reasons that will become apparent below). In this frame, the photon fluctuates into a hadronic system (a quark anti-quark colour triplet *dipole*, to lowest order in α_s) a long distance, $1/2m_T x \gg R_T$, upstream of the target. This system interacts briefly with the target and eventually the hadronic final state is formed. The formation time of the initial state hadronic fluctuations, and of the final state, is typically much longer than the interaction time with the target. This allows the process to be factorized into a wavefunction for the formation of the initial state, an interaction cross section with the target, and a wavefunction describing the formation of the final state. In this frame, the standard LT result of pQCD, at leading log accuracy, may be re-expressed using the following well-known interaction cross-section [14,18,19,31] for the scattering of the $q\bar{q}$ dipole with the target (for an explicit derivation see [32]):

$$\hat{\sigma}_{\text{pQCD}}(d_{\perp}^2, x) = \frac{\pi^2}{3} d_{\perp}^2 \alpha_s(\bar{Q}^2) x G^T(x, \bar{Q}^2). \quad (1)$$

which is a generalization of the two-gluon exchange model of [33] (see also references in [12]). Here d_{\perp} is the transverse diameter of the dipole, $x G^T$ is the leading-log gluon distribution of the target sampled at a scale $\bar{Q}^2 = \lambda/d_{\perp}^2$, with λ a logarithmic function of Q^2 . There are of course corrections, involving more complicated partonic configurations such as $q\bar{q}g$, which in general can not be described (except in special circumstances) using the interactions of dipoles of a given colour configuration. However, the description of small- x processes in

terms of an *interaction cross section* for the hadronic fluctuations of the photon remains a useful one.

For heavy nuclear targets, it is legitimate to neglect a logarithmic increase of the effective radius of the target with increasing energy. In this case there is, of course, a natural geometrical upper limit to the size of this inelastic interaction cross section given approximately by the transverse cross-sectional area of the target:

$$\hat{\sigma}_{\text{pQCD}} \leq \sigma_{\text{black}} = \pi R_T^2. \quad (2)$$

It seems plausible that small- x physics of the next generation of accelerators will be a combination of two generic phenomena, *generalised colour transparency* and *complete opacity* (absorption), which correspond to two different kinematical limits. In one limit, when x is fixed and $Q^2 \rightarrow \infty$, hard processes exhibit numerous colour transparency phenomena, which can be described in terms of various generalisations of the QCD factorization theorem. In another limit, when Q^2 is fixed and $x \rightarrow 0$, the interaction cross section increases with decreasing x (increasing energy), which leads to increased absorption by the target. Hence, in this kinematical limit, the approximation of complete absorption, which could naturally be termed “the black body limit (BBL)”, seems to be a promising guide to predict new distinctive hard QCD phenomena. Colour Transparency is a generic name used to describe the fact that small colourless configurations do not interact strongly with hadrons, which is reflected by the inclusion of the transverse diameter squared, d_\perp^2 , in (1). However, for a fixed dipole size (and neglecting for a moment an increase with increasing energy of the radius of a target which can be justified for heavy nuclear targets only), if the gluon density of the target continues to rise with increasing $1/x$, the interaction cross section will eventually reach its geometrical limit (cf. (2)). This is basically what is meant by complete opacity.

The validity of the BBL can be justified for DIS processes off heavy nuclear targets since contributions of colour transparency, and various peripheral phenomena (which complicate studies of BBL for nucleon targets) are suppressed. In the BBL, the nuclear structure function $F_2^A(x, Q^2)$ is predicted to behave as $R_A^2 Q^2 \ln 1/x$ with decreasing x , which is slower

than the x -behaviour predicted by the DGLAP evolution equations. Since the nucleon is “gray” rather than “black” as seen by the incoming high-energy fluctuation, peripheral effects are important and contribute to the total electron-nucleon DIS cross section (these effects lead to an increase of the essential impact factors with increasing energy). The nucleon structure function (gluon distribution) behave as $F_2^N(xG^N) \propto Q^2 R_N^2 \ln^3 1/x$ in the black body limit. In both the nuclear and nucleon cases, the expression for the total cross sections is a direct generalization of the Froissart unitarity limit [34] to DIS (see subsection III). One has to distinguish two features of these results. Firstly, the predicted Q^2 -independence of total cross sections grossly violates Bjorken scaling and serves as a very clean signal of the onset of the BBL regime. Secondly, the predicted energy (or x) dependence of the total electron-nucleon (but not electron-nucleus) cross section (nucleon structure functions) can probably be accommodated within the DGLAP LT pQCD framework by a suitable subtle re-tuning of the initial conditions (this has been the pattern in the era of HERA). Hence, it would be difficult to distinguish between the DGLAP and black body approximations and predictions thereof for the nucleon structure functions. A much more promising way to identify the BBL regime is to investigate the difference between the x dependence of nucleon structure function and the structure functions of heavy nuclei, as well as final states in DIS on nucleons and nuclei for which the BBL predicts several rather striking new phenomena.

By fixing Q^2 and decreasing x , one proceeds from the DGLAP regime to the BBL regime. Theoretical models attempting to quantify deviations from the DGLAP approximation and define the kinematical boundaries of the applicability of the DGLAP equations agree that the effects, which are responsible for the inapplicability of the DGLAP dynamics, are enhanced for nuclear targets by approximately a factor of $A^{1/3}$ if the approximation is made that the HT effects and nuclear shadowing of parton distributions are a correction [35]. Neglecting non-perturbative nuclear shadowing of the gluon distribution, one can estimate the ratio of the critical x at which the BBL regime sets in for DIS on nuclei and nucleon, as $x_A(\text{BBL})/x_N(\text{BBL}) \approx (A/2)^{1/(3n)}$ (the factor n comes from the energy dependence of the nucleon structure function F_2^N in the form $F_2^N \propto x^{-n}$). The factor $1/2$ in this relation ac-

counts for the difference between the nucleon radius, $r_N = 0.85$ fm, and a mean inter-nucleon distance in nuclei, $r_{NN} = 1.7$ fm.

Note that the complication of taking non-perturbative nuclear shadowing in nuclear parton distributions into account slightly reduces the advantage of using nuclear targets over nucleon ones for studying higher twist effects.

Since the DGLAP QCD evolution equations are leading twist equations, any violations of the DGLAP equation would signal a non-negligible role of higher twist effects. Therefore, a unique feature of electron-nucleus collisions is that by studying DIS on nuclear targets one can not only amplify the higher twist effects but also study them as a function of the target thickness (by varying nucleon number A).

In order to summarize the above discussion, we would like to re-emphasize that using nuclear beams in THERA has significant advantages over using a proton beam in studying new QCD phenomena such as the perturbative regime of very high parton densities and the transition from the DGLAP regime to black body scattering¹. Since these phenomena depend on the nucleon number, A , measurements of various observables as a function of A will be necessary. Fortunately this will be practical at THERA. The BBL interpretation of many phenomena, including the difference between the x -dependence of heavy nucleus and nucleon structure functions and some properties of final states, does not require knowledge of nuclear effects. It is clear that a consistent and complete interpretation of some experimental data would require reliable information about traditional nuclear effects at small x , primarily nuclear shadowing. However, as we shall explain in detail in Sect. V, using the profound connection between nuclear shadowing in inclusive electron-nucleus DIS and hard electron-proton diffraction, the QCD factorization theorem and modern fits to the diffractive data,

¹Formally, the notion of parton densities is defined in the leading twist approximation only. Thus, when discussing physics beyond the DGLAP approximation, one should be cautious and explicit in using the term “parton density”.

one can significantly reduce uncertainties in the predictions of the leading twist part of nuclear parton densities.

The rest of this section is organized as follows. The black body limit is discussed in Sect. III. We demonstrate that predictions made in the BBL are strikingly different from those obtained within the DGLAP approximation, especially for final states in DIS diffraction on nuclei. Precursors of the BBL can be studied by analysing the departure from the leading twist DGLAP evolution equation using the unitarity of the S -matrix for hard interactions as a guide. In Sect. IV, we discuss the relevant effects for a range of nuclei at central impact parameters. It is found that our predictions are sensitive to the amount of leading twist nuclear shadowing, which is considered in Sect. V. It is also demonstrated that in a wide range of x and Q^2 , leading twist shadowing dominates over higher twist shadowing, used frequently in eikonal-type models. After briefly considering experimental requirements in Sect. VI, we conclude in Sect. VII.

III. THE BLACK BODY LIMIT AND ITS SIGNALS IN DIS FINAL STATES

The leading twist (LT) approximation of perturbative QCD successfully describes DIS of photons on hadronic targets [5] and predicts a rapid increase² of structure functions with increasing energy (decreasing x). Within the LT approximation, there is no mechanism which would slow down or tame the rapid growth of the structure functions³.

However, it is clear that a rapid power-like growth of the structure functions (at a given impact parameter) cannot continue forever⁴ and, hence, the LT approximation must be

²This can be either introduced by hand at the initial evolution scale or generated by QCD evolution [36].

³One can show by direct pQCD calculations that the taming (shadowing) of parton densities at small x considered in eikonal and parton recombination models is a higher twist effect.

⁴At the same time, conventional nucleon structure functions integrated over all impact parameters

violated at very small x . Therefore, some higher-twist mechanism is required to explain the taming of the structure functions. A practical and almost model-independent approach to the taming of the structure function is based on the analysis of the unitarity of the S -matrix for the interaction of spatially small quark-gluon wave packets.

A. Unitarity and the black body limit

The most direct way to understand the constraints which are imposed by unitarity of the scattering matrix (for hadronic fluctuations of the virtual photon) on the nucleon and nucleus structure functions is to use the *impact-parameter representation* for the scattering amplitude. As explained in the introduction, in the target rest frame the incoming photon interacts with the target via its partonic fluctuations. Since the interaction time is much shorter than the life-time of the fluctuations at small x , the DIS amplitude can be factorised in three factors: one describing the formation of the fluctuation, another – the hard interaction with the target, and a final factor describing the formation of the hadronic final state. The $q\bar{q}$ dipole is the dominant fluctuation at short transverse distances, and we consider its interaction primarily in what follows.

Within this high-energy factorization framework the structure functions, F_L and F_T , may be written in the following simple way

$$F_{L,T}(x, Q^2) = \int dz d^2d_\perp |\psi_{L,T}^\gamma(z, d_\perp^2, Q^2)|^2 \frac{\text{Im } A(s, t = 0, d_\perp^2)}{s}, \quad (3)$$

where $\psi_{L,T}^\gamma(z, d_\perp^2, Q^2)$ are the light-cone wavefunctions of the longitudinally and transversely polarised virtual photon, respectively, z is the photon momentum fraction carried by one of the dipole constituents, s is the invariant energy of the dipole-target system ($s = (P + q)^2$ for the $q\bar{q}$ dipole), $t \approx -|\vec{q}_\perp|^2$ is the momentum transfer and d_\perp is the dipole's transverse diameter.

may increase with increasing energy even faster (according to the $\propto \ln^3 1/x$ law) than predicted by DGLAP.

The dipole-target scattering amplitude $A(s, t, d_\perp^2)$ can be expressed via the corresponding amplitude, $f(s, b, d_\perp^2)$, in impact-parameter, b , space ($b = b_\perp$ is Fourier conjugate to q'_\perp):

$$A(s, t, r^2) \equiv 2s \int d^2b e^{i\vec{q}' \cdot \vec{b}} f(s, b, r^2) . \quad (4)$$

The scattering amplitude $f(s, b, d_\perp^2)$ is related to the total cross section for the scattering of dipoles of fixed transverse diameter, d_\perp , by the optical theorem:

$$\sigma_{\text{tot}}(s, d_\perp^2) = 2 \int d^2b \text{Im} f(s, b, d_\perp^2) . \quad (5)$$

The unitarity of the scattering S -matrix [37] ($S_{ab} = \delta_{ab} + i f_{ab}$, $S_{ac}^\dagger S_{cb} = \delta_{ab}$) imposes the following conditions ⁵ on the scattering amplitudes (for each b , a continuum analogy of angular momentum in a partial wave analysis in non-relativistic quantum mechanics):

$$\text{Im} f_{aa}(s, b, d_\perp^2) = \frac{1}{2} (f_{aa}^\dagger f_{aa} + \sum_{c, c \neq a} f_{ac}^\dagger f_{ca}) , \quad (6)$$

where “a,c” are labels for definite states (on the right hand side we suppress the variables s, b, d_\perp for clarity). The first and second terms on the right hand side of (6) involve elastic and inelastic final states, respectively.

The black body limit (BBL) assumes that: (i) configurations with the impact parameters satisfying $b^2 \leq b_{\text{max}}^2$ are completely absorbed by target, i.e. the elastic matrix elements of the S -matrix are zero for those impact parameters: $S_{aa}(b \leq b_{\text{max}}) = \delta_{aa} + i f_{aa}(b \leq b_{\text{max}}) = 0$. This implies that $\text{Im} f_{aa}(s, b \leq b_{\text{max}}, d_\perp^2) = 1$, and leads to $|f_{aa}(s, b, d_\perp^2)|^2 = \sum_{c, c \neq a} |f_{ac}(s, b, d_\perp^2)|^2$ that is to the equality of the elastic and inelastic contributions to the total cross section. (ii) the region $b^2 \leq b_{\text{max}}^2$ gives the dominant contribution to the scattering

⁵A rather straightforward way to deduce unitarity of the S -matrix is to consider amplitudes for the scattering of bound states of fictitious heavy quarks Q and the prove that, for sufficiently large mass of the quarks M_Q and small x , dipole scattering would dominate. In order to complete the derivation, one also needs to use the fact that QCD is flavour blind if the resolution scales are chosen appropriately.

amplitude (5). The great advantage of the BBL is that calculations of the amplitudes of some small- x processes do not require specific model assumptions. Moreover, as will be discussed later, the BBL approximation seems to be realistic for DIS on heavy nuclear targets.

The dependence of $f(s, b, d_\perp^2)$ on the impact parameter, b , at large b follows from analytic properties of the scattering amplitude $A(s, t, d_\perp^2)$ in t -plane. A simple analysis leads to $f(s, b, d_\perp^2) = c \exp(-\mu b)$ at large b , where $c \propto x G^T(x, d_\perp^2) \propto 1/x^n$. Hence, following Froissart [34,37] we may evaluate the maximal impact parameter characterising the black body limit. One obtains $b_{\max}^2 \propto 1/\mu^2 \ln^2 1/x$ for a nucleon target, and $b_{\max}^2 = R_A^2$ for a heavy nuclear target (R_A being the radius of the nucleus). Note that the difference between b_{\max}^2 for the nucleon and nuclear case reflects the fact that the nucleon target is not a homogeneous sphere but rather an object with an extended diffuse edge.

Using these relationships, for the total dipole-nucleon scattering cross section (see also (5)) in the BBL approximation, one obtains

$$\hat{\sigma}_{\text{tot}}(s, d_\perp^2) = 2\pi(R_N^2 + 4c_N \ln^2 1/x). \quad (7)$$

In addition to the total cross section, one can examine the t -dependence of the cross section, corresponding to the amplitude in (4), defined through its slope, B :

$$\left. \frac{d \ln \sigma(s, t)}{dt} \right|_{t=0} = B = B_0 + 2\alpha'_{\text{eff}} \ln 1/x = \frac{\int d^2b b^2 f(s, b, d_\perp^2)}{2 \int d^2b f(s, b, d_\perp^2)}, \quad (8)$$

where $\alpha'_{\text{eff}} \equiv d(B/2)/d \ln 1/x$. We use above that the t -dependence of the real and imaginary parts of the amplitude is the same. In the BBL, one obtains

$$\begin{aligned} B &= \frac{b_{\max}^2}{4} = \frac{R_T^2}{4} + c_T \ln^2 1/x, \\ \alpha'_{\text{eff}} &= c_T \ln 1/x. \end{aligned} \quad (9)$$

Here R_T is the radius of the target, c_T is a factor which is similar for nucleon and nucleus targets. Hence for practical purposes, one can neglect c_T for heavy nuclear targets.

Finally, the proton structure function (at fixed Q^2) in the BBL reads

$$F_2^p(x, Q^2) \propto \sum_i e_i^2 Q^2 \frac{2\pi R_N^2}{12\pi^3} \left(1 + \frac{4c_N^2}{R_N^2} \ln^2 x_0/x\right) \ln 1/x. \quad (10)$$

Here the sum is taken over electric charges e_i of active quark flavours i . Note that the additional factor of $\ln 1/x$ in (10) as compared to (7) is due to the contribution of large masses resulting from the singular nature of the photon wavefunction. This reflects the logarithmic divergence of renormalization coupling constant for the electric charge (cf. (13) below). As one sees from (10), general principles of QCD and, in particular, the BBL approximation, do not exclude a fast ($\ln^3 1/x$) increase of the structure functions of a nucleon at $x \rightarrow 0$. In addition, the contribution from dipoles with the impact parameters larger than b_{\max} or sufficiently small dipoles (which are assumed to give a small contribution in the BBL approximation) should continue to increase with increasing energy as dictated by the DGLAP approximation of QCD. Thus, in practice, it would be very difficult, or even impossible, to distinguish the BBL prediction (10) from a similarly rapid growth predicted by the DGLAP equation and to search for saturation effects in inclusive nucleon structure functions. Hence, one should turn to DIS on nuclear targets in order to search for distinct signals of BBL dynamics.

The use of nuclei has two clear advantages. Firstly, scattering at large impact parameters, where the interaction is far from the BBL over a wide range of energies (the edge effects), is suppressed by the factor R_N/R_A . Secondly, in a broad range of impact parameters, $b \leq R_A$, the nuclear thickness is practically b -independent and much larger than in a nucleon. Hence, DIS on sufficiently heavy nuclei can serve as a good testing ground for the application of the BBL and will allow us to pinpoint some distinctive features of it. For example, as follows from the above discussion, the unitarity of S -matrix significantly tames the rapid growth of the nuclear structure functions and predicts the unitarity limit

$$F_2^A(x, Q^2) = \sum_i e_i^2 Q^2 \frac{2\pi R_A^2}{12\pi^3} \ln 1/4m_N R_A x . \quad (11)$$

Over the last few years a number of models, using the infinite momentum frame, were suggested in order to explain the dynamics of DIS at small x by building the nuclear wave function from large gluon fields and assuming a certain saturation of the parton densities (for the review and references see e.g., [38]). In many respects, these models and the BBL

approximation are similar.

The BBL in DIS from a heavy nucleus at small x was first considered by Gribov [39], before the discovery of QCD. Gribov assumed that each hadronic fluctuation of the virtual photon interacts with the target nucleus with the same maximal strength allowed by unitarity. Such an assumption, supported by the observed cross sections of hadron-nucleus interactions, was natural for understanding the dynamics of soft strong interactions in models predating QCD.

Thus, in the black body limit, DIS on nuclei is dominated by the dissociation of the incoming virtual photon into its hadronic fluctuations, which subsequently interact with the target with the same scattering cross sections $2\pi R_A^2$, and then hadronize into final states with mass M . The transverse and longitudinal nuclear structure functions may be conveniently formulated as an integral over produced masses

$$F_T^A(x, Q^2) = C \int_{M_{\min}^2}^{M_{\max}^2} dM^2 \frac{2\pi R_A^2}{12\pi^3} \frac{Q^2 M^2 \rho(M^2)}{(M^2 + Q^2)^2}, \quad (12)$$

$$F_L^A(x, Q^2) = C \int_{M_{\min}^2}^{M_{\max}^2} dM^2 \frac{2\pi R_A^2}{12\pi^3} \frac{Q^4 \rho(M^2)}{(M^2 + Q^2)^2}, \quad (13)$$

where $\rho(M^2) = \sigma^{e^+e^- \rightarrow \text{hadrons}}(M^2)/\sigma^{e^+e^- \rightarrow \mu^+\mu^-}(M^2)$. In the BBL, the coefficient $C = 1$.

The upper cutoff, $M_{\max}^2 \ll W^2 \approx 2q_0 m_N$, comes from the nuclear form factor:

$$-\frac{t_{\min} R_A^2}{3} \approx \frac{(M^2 + Q^2)^2}{4q_0^2} R_A^2/3 \approx m_N^2 x^2 \frac{R_A^2}{3} \ll 1. \quad (14)$$

The key element of the derivation of (13) is the observation that in the BBL, as a result of orthogonality of the wave functions of the eigenstates of QCD Hamiltonian with different energies, the non-diagonal transitions between states with different M^2 are zero. This enables one to write the structure functions as a single dispersive integral as is done in (13). Since (13) leads to a cross section for γ^*A scattering grossly violating Bjorken scaling ($\sigma_{\text{tot}}^{\gamma^*A}(x, Q^2) \propto \pi R_A^2 \ln(1/x)$ instead of $\propto 1/Q^2$), the BBL has been considered for some time to be an artifact of the pre-QCD physics. This is especially so since, within the parton model, the aligned jet model removed this gross scaling violation [40]. However, for consistency of the target rest frame and infinite momentum frame descriptions, an exponential

suppression with decreasing d_{\perp}^2 of the cross section of interaction of small-size configurations with hadrons was assumed to be required. This fact was subsequently explained and understood in terms of the QCD factorization theorem for the scattering of small dipoles, colour neutrality of the dipole and asymptotic freedom for hard processes in QCD (and the “suppression” was realised only to be only a single power in d_{\perp}^2 , cf. (1)).

In perturbative QCD, the dipole-target cross section (1), rapidly increases with increasing energy since the gluon density rapidly increases with decreasing x . Hence, if the increase of the interaction cross section is not tamed by some mechanism, it will reach values expected for the black body limit (i.e. tens of mb, cf. (2)).

Properties of the BBL in QCD are somewhat different from those within the Gribov picture due to a significant probability of smaller than average size configurations in the photon wave function, for which the conditions of the black body limit are not satisfied. As a result, the interaction of such small-size configurations is not tamed. Thus, in contrast to the Gribov approach, only a fraction of all configurations will interact according to the BBL approximation and therefore $C < 1$ in (13).

Using (1), it is straightforward to estimate the kinematical boundaries where the unitarity limits may be reached. Indeed, the requirement that $\sigma_{\text{el}} \leq \sigma_{\text{tot}}/2$ [18,25] (also assuming that (1) is applicable for the range of x in which the taming is necessary) indicates that for some gluon-induced hard processes the unitarity limit should be well within the reach of an electron-nucleus collider at HERA/THERA (for a review see [11]).

One can also make an interesting prediction about nuclear shadowing. Since the x -dependence of the nuclear structure function of (11) is significantly weaker than that for the proton structure function of (10), nuclear shadowing is not saturated (as is often assumed in the limit of fixed Q^2 and $x \rightarrow 0$), and we find

$$\frac{F_2^A(x, Q^2)}{AF_2^N(x, Q^2)} \propto \frac{R_A^2}{AR_N^2} \frac{1}{1 + 4c_N^2 R_A^2 \ln^2 1/x} . \quad (15)$$

However, at unrealistically small x , where the impact parameters become significantly larger than R_A , this effect will disappear.

In summary, since the contributions of small configurations (which have not reached the black body limit) remain significant in a wide range of x and Q^2 , studies of the total cross sections are a rather ineffective way to the search for the onset of the BBL regime. In particular, it may be rather difficult to distinguish the BBL from DGLAP approximation with different initial conditions in this way.

In what follows we shall demonstrate that studies of DIS final states provide a number of clear signatures of the onset of the BBL regime, which will be qualitatively different from the leading twist regime. For simplicity, we will assume that the BBL is reached for a significant part of the cross section and, hence, restrict our discussion to DIS on a large nucleus so that edge effects (which are important in the case of scattering off a nucleon) can be neglected.

B. Diffractive final states

The use of Gribov's orthogonality argument (to neglect non-diagonal transitions in (13)) allows the integrals over the masses to be removed in the expressions for the structure functions and, since diffraction is 50% of the total cross section in the BBL, we immediately find for the spectrum of diffractive masses:

$$\begin{aligned}\frac{dF_T^{D(3)}(x, Q^2, M^2)}{dM^2} &= \frac{\pi R_A^2}{12\pi^3} \frac{Q^2 M^2 \rho(M^2)}{(M^2 + Q^2)^2} , \\ \frac{dF_L^{D(3)}(x, Q^2, M^2)}{dM^2} &= \frac{\pi R_A^2}{12\pi^3} \frac{Q^4 \rho(M^2)}{(M^2 + Q^2)^2} .\end{aligned}\tag{16}$$

Moreover, the spectrum of hadrons in the centre of mass of the diffractively produced system should be the same as in e^+e^- annihilation. Hence, the dominant diffractively-produced final state will have two jets with a distribution over the centre of mass emission angle proportional to $1 + \cos^2 \theta$ for the transverse case and $\sin^2 \theta$ for the longitudinal case:

$$\frac{dF_T^{D(3)}(x, Q^2, M^2)}{dM^2 d \cos \theta} = \frac{3}{8} (1 + \cos^2 \theta) \frac{\pi R_A^2}{12\pi^3} \frac{Q^2 M^2 \rho(M^2)}{(M^2 + Q^2)^2} ,\tag{17}$$

$$\frac{dF_L^{D(3)}(x, Q^2, M^2)}{dM^2 d \cos \theta} = \frac{3}{4} \sin^2 \theta \frac{\pi R_A^2}{12\pi^3} \frac{Q^4 \rho(M^2)}{(M^2 + Q^2)^2} .\tag{18}$$

The transverse momentum of the jet, p_t , and the longitudinal fraction of photon energy, z , carried by the jet are related to the diffractive mass, M , and the angle, θ , as follows (we neglect here the quark masses as compared to Q, M):

$$\begin{aligned} p_t &= \frac{M}{2} \sin \theta , \\ z &= (1 + \cos \theta)/2 . \end{aligned} \tag{19}$$

Hence, in the BBL, diffractive production of high p_t jets is strongly enhanced:

$$\begin{aligned} \langle p_t^2(jet) \rangle_T &= 3M^2/20 , \\ \langle p_t^2(jet) \rangle_L &= M^2/5 . \end{aligned} \tag{20}$$

This is to be compared to the leading twist approximation where it is $\propto \ln Q^2$. The relative rate and distribution of the jet variables for the three jet events (originating from $q\bar{q}g$ configurations) will be also the same as in e^+e^- annihilation and hence is given by the standard expressions for the process $e^+e^- \rightarrow q\bar{q}g$ (see e.g. [41]).

An important advantage of the diffractive BBL signal is that these features of the diffractive final state should hold for $M^2 \leq Q_{BBL}^2$ even for $Q^2 \geq Q_{BBL}^2$ because configurations with transverse momenta $\leq Q_{BBL}/2$ still interact in the black regime (and correspond to transverse size fluctuations for which the interaction is already black).

Another interesting feature of the BBL is the spectrum of the leading hadrons in the virtual photon fragmentation region produced in DIS. The spectrum is essentially given by the θ -dependence of (17) and (18). For fixed M^2 , the jet distribution over z for transversely polarised photons is simply

$$\frac{d\sigma_T}{dz} \propto 1 + (2z - 1)^2 . \tag{21}$$

Similarly, for longitudinally polarised photons,

$$\frac{d\sigma_L}{dz} \propto z(1 - z) . \tag{22}$$

If no special separation procedure is undertaken, at small x one actually measures $\sigma_L + \epsilon\sigma_T$ (ϵ is the photon polarisation). In this case, combining (17) and (18) we find:

$$\frac{d(\sigma_T + \epsilon\sigma_L)}{dz} \propto \frac{M^2}{8Q^2}(1 + (2z - 1)^2) + \epsilon z(1 - z). \quad (23)$$

Exclusive vector meson production in the BBL is in a sense a resurrection of the original vector meson dominance model [42] without off-diagonal transitions. The amplitude for the vector meson-nucleus interaction is proportion to $2\pi R_A^2$ (since each configuration in the virtual photon interacts with the same BBL cross section). This is markedly different from the requirements [43] for matching generalised vector dominance model (see e.g., [44]) with QCD in the scaling limit, where the non-diagonal matrix elements are large and lead to strong cancellations. Hence, we can factorize out the cross section for the dipole interaction from the overlap integral between wavefunctions of virtual photon and vector meson to obtain for the dominant electroproduction of vector mesons

$$\begin{aligned} \frac{d\sigma^{\gamma_T^*+A \rightarrow V+A}}{dt} &= \frac{M_V^2}{Q^2} \frac{d\sigma^{\gamma_L^*+A \rightarrow V+A}}{dt} = \\ &= \frac{(2\pi R_A^2)^2}{16\pi} \frac{3\Gamma_V M_V^3}{\alpha(M_V^2 + Q^2)^2} \frac{4 |J_1(\sqrt{-t}R_A)|^2}{-tR_A^2}, \end{aligned} \quad (24)$$

where Γ_V is the electronic decay width $V \rightarrow e^+e^-$, α is the fine-structure constant, and $J_1(x)$ is the Bessel function. Thus the parameter-free prediction is that in the BBL at large Q^2 vector meson production cross sections have a $1/Q^2$ behaviour, in stark contrast to an asymptotic behaviour of $1/Q^6$ predicted in perturbative QCD [7,18,19].

In order to observe the onset of the BBL regime for a nucleon target, one should consider scattering at small impact parameters. However, a direct comparison of the BBL prediction for small b with data is very difficult since, in the BBL, the amplitude oscillates as a function of t . Also, in the case of a proton target, a significant nucleon spin-flip amplitude may mask these oscillations.

C. Inclusive spectra

In the leading twist approximation, the QCD factorization theorem is valid and leads to universal spectra of leading particles (independent of the target) for the scattering off partons

of the same flavour. Fundamentally, this can be explained by the fact that, in the Breit frame, the fast parton which is hit by the photon carries practically all of the photon's light-cone momentum ($z \rightarrow 1$). Due to QCD evolution, this parton acquires virtuality $\sim Q^2$, and a rather large transverse momentum, k_t (which is still $\ll Q^2$). So, in pQCD, quark and gluons emitted in the process of QCD evolution and in the fragmentation of highly virtual partons together still carry all the photon momentum. In contrast, in the BBL, configurations in which partons carry all of the photon momentum form only part of cross section of leading hadron production. Another part is from inelastic collisions of configurations where all partons carry appreciable momentum fractions and large relative transverse momenta (these configurations are rather similar to the case of diffractive scattering (see e.g. (17) and (18))). Hence, in the BBL case, the spectrum of leading hadrons (in the direction of the virtual photon) is expected to be much depleted.

The inclusive spectrum of leading hadrons can be estimated as due to the independent fragmentation of quark and antiquark of virtualities $\geq Q^2$, with z and p_\perp distributions given by (17) and (18) (cf. the case of diffractive production of jets discussed above). The independence of fragmentation is justified because large transverse momenta of quarks dominate in the photon wave function (cf. eqs. (17, 18, 19) and because of the weakness of the final state interaction between q and \bar{q} , since the α_s is small and the rapidity interval is of the order of one. Obviously, this leads to a gross depletion of the leading hadron spectrum as compared to the leading twist approximation situation where leading hadrons are produced in the fragmentation region of the parton which carries essentially all momentum of the virtual photon ⁶. Taking the production of multi-jet states like $q\bar{q}g$ into account will further enhance this scaling violation. If we neglect gluon emissions in the photon wave function,

⁶Qualitatively, this pattern is similar to the one expected in the soft region since the spectrum of hadrons produced in hadron-nucleus interactions is much softer than for hadron-nucleon interactions.

we find, for instance:

$$\frac{dN_{T^*/h}^*}{dz} = 2 \int_z^1 D^{q/h}(z/y, Q^2) \frac{3}{4} (1 + (2y - 1)^2) dy, \quad (25)$$

for the total differential multiplicity of leading hadrons produced by transversely polarised virtual photons, in the BBL. $D^{q/h}(z/y, Q^2)$ is the fragmentation function of a quark with flavour q into the hadron h . Here we use that $D^{u/h}(z/y, Q^2) = D^{d/h}(z/y, Q^2)$ and neglect a small difference in the fragmentation functions of light and heavy quarks.

An illustration of the results of the calculation of $dN_{T^*/h}^*/dz$ is presented in Fig. 1. We normalise the distribution to the leading twist case by using realistic up-quark fragmentation functions at $Q^2 = 2 \text{ GeV}^2$ [45] (the up and down quark distributions are similar and we neglect the small difference induced by including further flavours). One can see from the figure that a gross violation of the factorization theorem is expected in the BBL. The spectrum of leading hadrons is much softer at large z , with an excess multiplicity at $z \leq 0.1$. Note that the use of leading twist fragmentation functions in the above expression probably underestimates absorption. So the curve in Fig.1 can be considered as a conservative lower limit for the amount of suppression.

With an increase of Q^2 we expect a further softening related to a change in the partonic structure of the virtual photon wave function. Progressively more configurations contain extra hard gluons, which fragment independently in the BBL, further amplifying deviations from the standard leading twist predictions.

Another important signature of the BBL is the change of p_t distributions with decreasing x (at fixed Q^2). The spectrum of the leading hadrons should broaden due to increased p_t of the fragmenting partons. Hence, the most efficient strategy would be to select leading jets in the current fragmentation region and examine the z and p_t -dependence of such jets. Qualitatively, the effect of broadening of p_t -distributions is similar to the increase of the p_t distribution in the model [46], although final states in DIS were not discussed in this model.

An important advantage of inclusive scattering off a nucleus is the possibility to use a centrality trigger. For example, one could use the number of nucleons emitted in the

nucleus decay (soft nucleons in the nucleus rest frame) to select scattering at the central impact parameters. Such a selection allows the effective thickness of the nucleus to be increased, as compared to the inclusive situation, by a factor ~ 1.5 and, hence, allows for the BBL to be reached at significantly larger x . The signal for the BBL will be a change of the spectrum with centrality of the collisions, in contrast to the LT case where no such correlation is expected. Note that the lack of absorption of leading particles in DIS off nuclei at the fixed target energies and $Q^2 \geq 2 \text{ GeV}^2$ is well established experimentally, see e.g. [47].

To summarise, predictions for a number of simple final state observables in the black body limit are distinctly different from those made in the leading twist approximation and, hence, will provide model-independent tests of the onset of the BBL.

IV. UNITARITY CONSTRAINTS FOR ELECTRON-NUCLEUS DIS

While predictions for inclusive DIS and DIS final state observables in the BBL are distinct, one still would like to determine the kinematical region where the regime of the BBL sets in. One way to address this issue is to examine the unitarity of the S -matrix for the interactions of purely perturbative QCD fluctuations.

A. The interaction of small colour dipoles with hadrons

The dipole picture of electron-target DIS is valid when the lifetime of the fluctuation is much longer than the interaction time with the target. Equally, this relation may be expressed in terms of the *coherence length*, l_{coh} , of the fluctuation (relative to the target radius). This length is given by the average longitudinal distances (Ioffe distances) in the correlator of the electromagnetic currents which determine the structure function $F_2(x, Q^2)$. A simple analysis shows that $l_{coh} \sim 1/(2m_N x)$. At HERA l_{coh} can reach values of 10^3 fm (for moderate Q^2 only). As Q^2 increases, the scaling violations lead to a gradual reduction of l_{coh} at fixed x and ultimately to the dominance of longitudinal distances $\sim R_N$ (for a discussion see [11]).

In the target rest frame, when l_{coh} is sufficiently large, the virtual photon can fluctuate into a variety of partonic configurations containing various numbers of partons and involving different transverse sizes. The simplest is a $q\bar{q}$ dipole, which dominates at very small distances. Since under $SU(3)_c$ transformations the quark and the anti-quark transform in the fundamental representation (like 3 and $\bar{3}$) the name “colour triplet” is often used for the $q\bar{q}$ pair (although overall its colour is of course neutral). The $q\bar{q}$ -dipole of a small diameter interacts with a hadronic target with an interaction cross section given by (1). Another important photon fluctuation is the one consisting of a quark, anti-quark and gluon, with a relatively large transverse momentum between the quark and the anti-quark. Such configurations effectively transform in the adjoint representation (effectively 8, $\bar{8}$) and so are known as the $q\bar{q}g$ colour octet dipole. There are of course other $q\bar{q}g$ configurations, for example those in which the gluon and either the quark or anti-quark have a large relative transverse momentum (these merely correspond to the $\mathcal{O}(\alpha_s)$ corrections to the colour triplet dipole) and other more general configurations which do not correspond to dipoles at all.

For the case of scattering of colour octet dipoles off a target, the corresponding cross section is enhanced a colour factor (given by the ratio of the Casimir operators of $SU(3)_c$), $C_F(8)/C_F(3) = 9/4$ [25,32,48]:

$$\begin{aligned}\hat{\sigma}_{\text{pQCD}}^{\text{octet}}(d_{\perp}^2, x) &= \frac{9}{4} \hat{\sigma}_{\text{pQCD}}^{\text{triplet}}(d_{\perp}^2, x) \\ &= \frac{3\pi^2}{4} d_{\perp}^2 \alpha_s(\bar{Q}^2) x G_T(x, \bar{Q}^2) .\end{aligned}\tag{26}$$

Both (1) and (26) predict cross sections steeply rising with increasing energy (driven by the rise of the gluon density with decreasing x). Fitting the energy dependence in the form ⁷ $\sigma_{\text{pQCD}}(s, Q^2) \propto s^{n(Q^2)}$, one finds

$$n(Q^2 = 4 \text{ GeV}^2) \approx 0.2 ,$$

⁷Such fit is useful in practical applications. Perturbative QCD predicts the behaviour $\propto a + b \ln 1/x + c \ln^2 1/x$ for the HERA energy range since radiation of ≤ 1 -2 hard gluons is possible in the multi Regge kinematics at HERA.

$$n(Q^2 = 40 \text{ GeV}^2) \approx 0.4 . \quad (27)$$

One of the manifestations of the behaviour predicted by (27) is the Q^2 -behaviour of the measured exclusive vector meson production. The interaction cross sections of (1) and (26) may be thought of as a complimentary description of the physics described by the leading log QCD evolution equations at small x . However, an accurate determination of the relation between \bar{Q}^2 and the transverse size d_\perp in these equations requires a next-to-leading order QCD analysis in this framework which has not been done yet. Numerical studies [19,31] based on matching of the d_\perp -space and Q -space expressions for $\sigma_L(x, Q^2)$, lead to $\lambda \sim 9 - 10$ for a sufficiently broad range of Q^2 and x . With this choice of λ , a good description of the recent inclusive DIS electron-proton data was obtained (with a suitable extrapolation to large d_\perp [31]) without any further fitting. As already mentioned, λ is a logarithmically-decreasing function of the dipole size d_\perp . In particular, at large values of d_\perp , $d_\perp \geq 0.3$ fm, where connection between d_\perp^2 and Q^2 is rather sensitive to non-perturbative effects, one expects a decrease of λ with increasing d_\perp^2 . On the other hand, it was found that variations in λ do not significantly effect values of $\hat{\sigma}_{\text{pQCD}}(d_\perp^2, x)$. Hence, our following estimates of the unitarity constraints, which are made using (1) and (26), are insensitive to a possible decrease of λ at large d_\perp^2 .

B. Unitarity constraints

The rapid increase of the cross sections given in (1) and (26) with decreasing x cannot continue forever, otherwise the unitarity of the S -matrix will be violated (see (6)). The unitarity boundary $\text{Im } f(s, b, d_\perp^2) = 1$ can be expressed in terms of the pQCD dipole cross section as

$$\hat{\sigma}_{\text{pQCD}}^{\text{inel}} = \sigma^{\text{el}} = \sigma^{\text{tot}}/2 , \quad (28)$$

and is applicable to any hadronic target. For a nucleus, with the atomic number A , $\hat{\sigma}_{\text{pQCD}}^{\text{inel}}$ cannot exceed its geometric limit πR_A^2 . Thus, generalising (1) and (26) for a nuclear target,

we obtain the following kinematical restrictions imposed by the unitarity of the S -matrix for $x \ll 1/4R_A m_N$:

$$\begin{aligned}\sigma_A^{q\bar{q}}(d_\perp^2, x) &= \frac{\pi^2}{3} d_\perp^2 \left[xG^A(x, \bar{Q}^2) \right] \alpha_s(\bar{Q}^2) \lesssim \pi R_A^2, \\ \sigma_A^{q\bar{q}g}(d_\perp^2, x) &= \frac{3\pi^2}{4} d_\perp^2 \left[xG^A(x, \bar{Q}^2) \right] \alpha_s(\bar{Q}^2) \lesssim \pi R_A^2, \end{aligned} \quad (29)$$

where $xG^A(x, \bar{Q}^2)$ is the nuclear gluon density. The kinematical boundaries following from these equations are presented as curves in the x - \bar{Q} plane in Figs. 14-17 of [11].

The unitarity constraints are even more stringent for DIS on nuclei at central impact parameters b , $b \leq R_A$. This is essentially equivalent to scattering off a cylinder of the length $2R_A$ oriented along the reaction axis. Obviously, in this case, edge effects are suppressed and one also gains an additional factor of ~ 1.5 on the left hand side of (29) due to the increased density of nucleons. The nuclear gluon distribution at a given impact parameter b is introduced as [49]

$$xG^A(x, Q^2, b) \equiv A xG^N(x, Q^2) f^A(x, Q^2, b) T^A(b), \quad (30)$$

where the function $f^A(x, Q^2, b)$ describes the amount of nuclear shadowing, $T^A(b) = \int_{-\infty}^{\infty} dz \rho^A(b, z)$ and $\int d^2b T^A(b) = 1$. Note that nuclear shadowing is larger at central impact parameters than in the situation when one averages over all impact parameters. Now, the unitarity constraints for DIS on nuclei at central impact parameters immediately follow from (29) for colour triplet

$$1.5 \times \frac{\pi^2}{3} r^2 \left[xG^A(x, \bar{Q}^2, b=0) \right] \alpha_s(\bar{Q}^2) \lesssim \pi R_A^2, \quad (31)$$

and colour octet dipoles

$$1.5 \times \frac{3\pi^2}{4} r^2 \left[xG^A(x, \bar{Q}^2, b=0) \right] \alpha_s(\bar{Q}^2) \lesssim \pi R_A^2. \quad (32)$$

The kinematical regions prohibited by these unitarity constraints (defined by $x < x_{\text{lim}}, \bar{Q} < Q_{\text{eff}}$) lie to the left of the curves in Figs. 2 and 3 (on the boundary $\bar{Q} \equiv Q_{\text{eff}}, x \equiv x_{\text{lim}}$). For the nucleon gluon density we used the CTEQ4L [50] parameterization evaluated at the scale

$Q^2 = 4 \text{ GeV}^2$. For each nucleus, we present scenarios with the highest and lowest shadowing (see Sect. V). The curves with more shadowing lie below the ones with less shadowing, for all Q^2 . To illustrate the trends given by (31), the curves are extended to the region $x \geq 1/(4R_A m_N)$ where, strictly speaking, the unitarity constraints (of (31) and (32)) should not be directly applied.

As one can see from Figs. 2 and 3, effects associated with the unitarity constraints are expected, in a wide range of x and Q^2 , to be covered by THERA. Regardless of the nature of such effects, strong modifications of the gluon field in heavy nuclei (as compared to the incoherent sum of the nucleon fields) appear to be unavoidable.

In summary, in the search for the BBL we observe that employing nuclear targets allow us to gain substantially in the region where higher twist effects become important. However, the presence of the leading twist nuclear shadowing reduces the magnitude of this gain. It is very important that in a wide range Q^2 the unitarity limit is reached at relatively large x so that $\ln Q^2/\Lambda_{\text{QCD}}^2$ is comparable to $\ln x_0/x$ (where $x_0 \sim 0.05$ is the starting point for the gluon emission in the $\ln 1/x$ evolution). Hence, the diffusion to the small transverse momenta is likely to be a correction. Therefore non-perturbative QCD, with a large coupling constant, is unlikely to be relevant for the taming of the structure functions.

V. NUCLEAR SHADOWING AND DIFFRACTION

A long time ago Gribov [51] established an unambiguous connection between the cross section of small- t diffraction of a hadron off a nucleon and the amount of shadowing in the interaction of the same hadron with a nucleus, for the limit in which only two nucleons of the nucleus are involved. Applying Gribov's formulae to describe photon-deuteron scattering, the effect of nuclear shadowing for the total cross section can be expressed ⁸ as [52]

⁸ The contribution of the real part of the diffractive scattering amplitude was neglected in [51] since it was assumed that the total cross section is energy-independent.

$$\sigma_{\text{shad}} = \frac{\sigma_{\text{tot}}(eD) - 2\sigma_{\text{tot}}(ep)}{\sigma(ep)} = \frac{(1 - \lambda^2)}{(1 + \lambda^2)} \frac{\frac{d\sigma_{\text{diff}}(ep)}{dt}|_{t=0}}{\sigma_{\text{tot}}(ep)} \frac{1}{8\pi R_D^2}, \quad (33)$$

where λ is the ratio of real to imaginary parts of the amplitude for diffractive DIS, and R_D is the deuteron radius. For small x , λ may be as large as $0.2 \div 0.3$, which results in $(1 - \lambda^2)/(1 + \lambda^2) \sim 0.8 \div 0.9$. For simplicity, we have neglected the longitudinal nuclear form factor (which leads to a cutoff of the integral over the produced masses, cf. e.g., (13))

It is worth emphasising that (33) does not require the dominance of the leading twist in diffraction. The only assumption, which is due to a small binding energy of the deuteron and which is also known to work very well in calculations of hadron-nucleus total and elastic cross sections, is that the nucleus can be described as a multi-nucleon system⁹. Under these natural assumptions, one is essentially not sensitive to any details of the nuclear structure, such as short-range nucleon correlations, etc.

A. Inclusive diffraction at HERA and predictions for nuclear parton densities

The Gribov approximation has been applied to the description of shadowing in nuclear DIS for a long time. The first calculations were performed in [54,55] before the advent of HERA and, hence, required modelling of diffraction in DIS. This modelling was based on the QCD extension of the Bjorken aligned jet model [54], and produced a reasonable description of the NMC data [56]. More recently, an explicit use of the HERA diffractive data allowed an essentially parameter-free description of these data [57] to be provided.

Two important features of the HERA inclusive diffractive data [58,59] are the approximate Bjorken scaling for the diffractive parton densities and a weak dependence of the total

⁹The condition that the matrix element $\langle A|T[J_\mu(y), J_\nu(0)]|A \rangle$ (which defines the nuclear structure function and total cross section) involves only nucleonic initial and final states is not so obvious in the infinite momentum frame. However, it is implemented in most of the light-cone models [35,53].

probability of diffraction P_{diff} on Q^2 : $P_{\text{diff}} \sim 10\%$ at $Q^2 \geq 4 \text{ GeV}^2$. The first observation is in line with the Collins factorization theorem [60] which states that in the Bjorken limit, the diffractive structure functions $f_j^D(\beta, Q^2, x_{\mathbb{P}}, t)$ satisfy the DGLAP evolution equations ($\beta = x/x_{\mathbb{P}} \approx Q^2/(Q^2 + M^2)$ and $x_{\mathbb{P}} \approx (M^2 + Q^2)/2q \cdot (p - p')$ is the fraction of the proton's momentum carried by the diffractive exchange).

A relatively small value of the probability of diffraction (as compared to the case of πN scattering) indicates that the average strength of the interaction leading to diffraction is correspondingly small. To characterise this strength it is instructive to treat diffraction in the S -channel picture using the eigenstates of the scattering matrix [61]. Such an approach is complementary to the picture of the factorization theorem. The use of the optical theorem leads to the following definition of the effective strength of the interaction (for diffraction in nucleon collisions and shadowing in nuclear collisions):

$$\sigma_{\text{eff}}^j(x, Q^2) \equiv 16\pi \frac{\frac{d\sigma_{\text{diff}}^j}{dt}|_{t=0}}{\sigma_{\text{tot}}^j(x, Q^2)} . \quad (34)$$

Here the superscript j indicates which hard parton is involved in the elementary hard process of the cross section $\sigma_{\text{tot}}(x, Q^2)$. This equation allows the average cross section for configurations which contribute to quark-induced and gluon-induced diffraction to be extracted.

Recently a number of phenomenological analyses of HERA inclusive diffractive and diffractive jet production data were performed within the leading twist approximation for hard diffraction. We have compared several of these analyses [58,62,63] and found that they lead to fairly similar values of σ_{eff}^j , especially if a matching at large diffractive masses to the soft factorization was implemented (for details see [64]).

The results for σ_{eff}^j for up quarks and gluons are presented in Fig. 4. We used results of two analyses of the HERA diffractive data (by the H1 collaboration [58], labelled by “H1” in the figure, and by Alvero *et al.* [62], labelled by “ACWT+”). The diffractive parton densities of [62] were extended to the region of small β by requiring consistency with the soft factorization theorem. Three curves (solid, dashed and dotted) represent the Q^2 -evolution of σ_{eff}^j . While the Q^2 -evolution is not very significant for σ_{eff}^u of the up quark, it decreases

σ_{eff}^g rather rapidly for gluons. This rapid change is explained by large scaling violations for $xG^N(x, Q^2)$.

Combining the Gribov theory with the Collins factorization theorem and comparing the QCD diagrams for hard diffraction and for nuclear shadowing arising from the scattering off two nucleons (see Fig. 5), one can prove [65] that, in the low thickness limit, the leading twist nuclear shadowing is unambiguously expressed through the diffractive parton densities $f_j^D(x/x_P, Q^2, x_P, t)$ of ep scattering:

$$f_{j/A}(x, Q^2)/A = f_{j/N}(x, Q^2) - \frac{1}{2} \frac{1 - \lambda^2}{1 + \lambda^2} \int d^2b \int_{-\infty}^{\infty} dz_1 \int_{z_1}^{\infty} dz_2 \int_x^{x_0} dx_P \times \rho_A(b, z_1) \rho_A(b, z_2) \cos(x_P m_N(z_1 - z_2)) f_{j/N}^D(\beta, Q^2, x_P, t) \big|_{k_t^2=0}, \quad (35)$$

where $f_{j/A}(x, Q^2)$ and $f_{j/N}(x, Q^2)$ are the inclusive parton densities, ρ_A is the nucleon density in the nucleus. At moderately small values of x , one should also add a term related to the longitudinal distances comparable to the inter-nucleon distances in the nucleus. This additional term can be evaluated using information on the enhancement of the gluon and valence quark parton densities at $x \sim 0.1$ at the initial scale Q_0^2 . This would slightly diminish nuclear shadowing at higher Q^2 via the Q^2 evolution. To summarise the results of (35), the nuclear shadowing effect given by $(1 - f_{j/A}(x, Q^2)/A f_{j/N}(x, Q^2))$, is proportional to $\sigma_{\text{eff}}^j(x, Q^2)$.

For $N \geq 3$ nucleons, we need to establish which configurations in the photon wavefunction dominate in diffraction. There are two extreme alternatives, i.e. a dominance of either hadronic-size configurations (as indicated by the aligned jet model) or of small size ($\sim 1/Q$) fluctuations. Figure 6 represents the corresponding diagrams (contributing to nuclear shadowing).

One can determine which of these extremes is closer to reality by comparing the effective cross section characterising diffraction (34) with the cross section, $\sigma_{\text{pQCD}}(d_{\perp}^2, x)$, for the double interaction of a dipole with a small and fixed diameter $d_{\perp} \sim 1/Q$, within the eikonal approach, given by (1). Thus, for the x -range studied at HERA at $Q^2 \geq 4 \text{ GeV}^2$ ($x \sim 0.001$), large-size configurations dominate, while the small dipoles contribute little to the bulk of

the inclusive diffractive cross section. This can also be seen from a comparison of the amount of nuclear shadowing in F_L^A calculated within the leading twist and eikonal approaches. This is consistent with the experimental observation that the t -slope of the inclusive diffraction ($B \sim 7 \text{ GeV}^{-2}$) is significantly larger than for the processes where small-size dipole dominate ($B \sim 4.5 \text{ GeV}^{-2}$). At lower $x \sim 10^{-4}$, small dipoles may become much more important due to the increase of $\hat{\sigma}_{\text{pQCD}}$ due to the QCD evolution.

It is well known that total, elastic and inelastic diffractive cross sections for the interactions of hadrons with nuclei are quantitatively well-described within the scattering eigenstate approximation [61], which is a generalization of the eikonal approximation. Since, at $Q^2 = 4 \text{ GeV}^2$, relatively soft interactions give the dominant contribution to diffraction, interactions with $N \geq 3$ nucleons can be considered using a generalised eikonal model with an effective cross section given by (34). We found that, due to a relatively small value of σ_{eff}^q , the amount of nuclear shadowing for F_2^A is relatively modest (as compared to the nuclear gluon distribution) and is practically independent of fluctuations of the effective cross section (when σ_{eff} is kept fixed) [66]. The Q^2 -dependence of shadowing is taken into account via the DGLAP evolution equations. Recently, we performed an extensive comparison of different parametrisations of the diffractive structure functions [64]. The results will update the analysis [65] to include a range of modern parameterizations of the quark and gluon diffractive parton densities. Using the effective cross sections presented in Fig. 4 and generalising (35) to include the rescattering terms with $N \geq 3$ nucleons, we are able to produce predictions for up quark and gluon parton distributions for a number of nuclei. As an example Fig. 7 represents the ratio of nuclear to nucleon up quark and gluon parton distributions for nuclei of ^{12}C (carbon) and ^{206}Pb (lead). Note that since the models we used provide good fits to the HERA diffractive data for $F_2^D(x, Q^2, x_P)$, they effectively take into account higher twist terms, if they are present in the data.

Hence, we conclude that combining the Gribov theory with the factorization theorem for inclusive diffraction and experimental information from HERA provides reliable predictions for nuclear parton distributions and, hence, for F_2^A in the HERA and THERA experimental

ranges.

B. Gluon shadowing

We explained above that since the interaction of the colour octet dipole is enhanced by a factor $9/4$ relative to a colour triplet [32,25,48], one expects, for processes sensitive to such configurations, an earlier onset of the regime where unitarity effects may become important.

The leading twist mechanism of nuclear shadowing is connected to the amount of the leading twist diffraction in gluon-induced reactions. The larger strength of the perturbative interaction as well as stronger non-perturbative interactions up to a scale ~ 2 GeV in the gluon channel suggest that the gluon-induced diffraction should occur with a large probability.

This is consistent with another interesting feature of the current HERA diffractive data (shared by the diffractive data from the proton colliders), i.e. a very important role of the gluons in hard diffraction. In the language of the diffractive community, the “perturbative Pomeron” is predominantly built of gluons. To quantify this statement it is convenient to define the probability of diffraction for a hard probe which couples to a parton j [65]:

$$P_j(x, Q^2) = \frac{\int dt dx_P f_j^D(x/x_P, Q^2, x_P, t)}{f_j(x, Q^2)}. \quad (36)$$

A large probability of diffraction in the gluon channel:

$$\begin{aligned} P_g(x \leq 10^{-3}, Q^2 = 4 \text{ GeV}^2) &\sim 0.4, \\ P_g(x \leq 10^{-3}, Q^2 = 10 \text{ GeV}^2) &\sim 0.2, \end{aligned} \quad (37)$$

leads via (36) to a large σ_{eff}^g (see Fig. 4) and, hence, to the prediction of a *large leading twist shadowing* for $G^A(x \leq 10^{-2}, Q^2)$ (see Fig. 7). Interactions of small dipoles are more important in the gluon case than in the quark case. Nevertheless, if we use the eikonal approximation (in the same spirit as for $q\bar{q}$ dipoles) to estimate the relative importance of

the leading and higher twist effects, we find that up to fairly small x in a wide range of Q^2 , the leading twist terms dominate. Note that in this case one should use $\sigma_{q\bar{q}N}$ from [31] rescaled by the factor 9/4 even for the dipole sizes where non-perturbative effects could be important. A comparison of Figs. 2 and 3 suggests that the higher twist effects appear to be more important in the gluon channel than in the quark channel. Also, the gluon induced interactions of a projectile with several nucleons are much more important and more sensitive to details of the interaction dynamics. However, with $\sigma_{\text{eff}}^g \sim 40$ mb, a large leading twist shadowing in the gluon channel appears to be unavoidable. It seems to be large enough to reduce strongly the gluon densities. However, even this strong reduction can not prevent the violation of unitarity for the interaction of colour octet systems with heavy nuclei, as can be seen from Fig. 3. For scattering at central impact parameters, this may already occur at $Q \sim 2$ GeV for the whole x range, $x \leq 1/(4m_N R_A)$.

C. Shadowing in the interaction of small dipoles with nuclei

For several small- x processes, we can probe the interactions of a small colour dipole with the nucleus directly. These include $\sigma_L(x, Q^2)$, $\sigma(\gamma + A \rightarrow J/\psi + A)$ and $\sigma(\gamma_L^* + A \rightarrow \rho + A)$.

We argued above that the eikonal approximation for fixed small d_\perp leads to much weaker absorption effects than the leading twist shadowing. The eikonal approach is also inconsistent with the QCD factorization theorem for the production of vector mesons [8] which leads at small x to [7]

$$\frac{\frac{d\sigma}{dt}(\gamma_L^* A \rightarrow V A)|_{t=0}}{\frac{d\sigma}{dt}(\gamma_L^* N \rightarrow V N)|_{t=0}} \approx \left[\frac{F_L^A(x, Q)}{F_L^N(x, Q)} \right]^2 \approx \left[\frac{xG^A(x, Q)}{xG^N(x, Q)} \right]^2. \quad (38)$$

Another observable sensitive to the difference between the leading twist and eikonal approaches is F_L^A . It can be expressed via nuclear parton distributions (we consider the leading order in α_s expression):

$$F_L^A(x, Q^2) = \frac{2\alpha_s(Q^2)}{\pi} \int_x^1 \frac{dy}{y} (x/y)^2 \left(\sum_{i=1}^{n_f} e_i^2 (1 - x/y) y G^A(y, Q^2) + \frac{2}{3} F_2^A(y, Q^2) \right). \quad (39)$$

The amount of nuclear shadowing for σ_L^A can be expressed by the ratio

$$\frac{F_L^A}{AF_L^N} = \frac{\int_x^1 \frac{dy}{y} (x/y)^2 \left((1 - x/y) \sum_i e_i^2 y G^A(y, Q^2) + 2F_2^A(y, Q^2)/3 \right)}{A \int_x^1 \frac{dy}{y} (x/y)^2 \left((1 - x/y) \sum_i e_i^2 y G^N(y, Q^2) + 2F_2^N(y, Q^2)/3 \right)}. \quad (40)$$

Results using (40) are presented in Fig. 8 for the same parameterizations as in the previous figures.

The impact-parameter eikonal approximation for $x \ll 1/(4m_N R_A)$ (where finite coherence length effects, which cannot be unambiguously treated in the eikonal approximation, can be safely neglected), leads to substantially smaller shadowing for the interaction of small dipoles (see Fig. (15) of [18]). The cleanest way to observe this effect would be to study coherent J/ψ production. THERA would be able to cover a broad range of $x = (M_{J/\psi}^2 + Q^2)/W^2$ starting from the region of colour transparency (amplitude proportional to nucleon number A) and extending to the colour opacity regime where there is a strong reduction of the amplitude (see Fig. 9).

D. Total cross section of coherent inclusive diffraction

There is a deep connection between shadowing and the phenomenon of diffractive scattering off nuclei. The simplest way to investigate this connection is to apply the AGK cutting rules [67]. Several processes contribute to diffraction on nuclei: (i) coherent diffraction in which the nucleus remains intact, (ii) break-up of the nucleus (without producing of hadrons in the nucleus fragmentation region), (iii) rapidity gap events (with hadron production in the nucleus fragmentation region). In [52] we found that for $x \leq 3 \cdot 10^{-3}$, $Q^2 \geq 4 \text{ GeV}^2$, the fraction of the DIS events with rapidity gaps reaches about 30-40% for heavy nuclei, with a fraction of the events of type (iii) decreasing rapidly with A . Recently, together with M. Zhalov one of us (MS) investigated the dependence of the fraction of the events due to coherent diffraction and due to the break-up of the nucleus on the strength of the interaction, σ_{eff}^j . We found that this fraction increases with σ_{eff}^j rather slowly. Thus, it is not sensitive to fluctuations of σ_{eff} . One can see from Fig. 10 that one expects a significantly smaller fraction for quark-induced processes ($\approx 35\%$) of coherent events than for gluon-induced processes

($\approx 45\%$). We also found that the ratio of diffraction with and without nuclear break-up is small (10-20%) in a wide range of nuclei, and weakly depends on σ_{eff} . Hence, it would be pretty straightforward to extract coherent diffraction by simply using anti-coincidence with a forward neutron detector, especially in the case of heavy nuclei (see discussion in [68]).

It is worth emphasising that the proximity of $\sigma_{\text{el}}/\sigma_{\text{tot}}$ to $1/2$ does not necessarily imply the proximity of the BBL in the sense of hard physics (it may also occur in the soft aligned-jet type scenario). A key distinction in this regard is in the dominance of the dijet production, broadening of the p_t distributions, etc, as discussed in Sect. III.

Other manifestations of leading twist shadowing include a strong A -dependence of the fluctuations of the central multiplicity distribution of the produced hadrons [52], and strong modifications of the leading hadron spectrum [65] for rapidities where the diffractive contribution is small. This is also in marked contrast to the black body limit, where major modifications occur already at the highest rapidities.

VI. EXPERIMENTAL CONSIDERATIONS

The expected nuclear effects in the small- x region are large enough so that measurements of the ratios of the corresponding quantities for electron-nucleus and electron-nucleon scattering with an accuracy of only a few percent will be sufficient. Hence, the luminosities required for the first run of measurements are rather modest. The estimates of [69] indicate that luminosities of about 1 pb^{-1} per nucleus would be sufficient for measurements of a number of important inclusive observables which include ratios of the structure functions, the A -dependence of global features of diffractive cross sections, ratios of the leading particle spectra and fluctuations of the multiplicity in the central rapidity range. Luminosities of the order of 10 pb^{-1} per nucleus will be necessary to measure gluon densities via $2 + 1$ jet events directly, to observe the pattern of colour opacity in exclusive vector meson production and to establish differential diffractive parton densities of nuclei.

Requirements for the detector are practically the same as for the study of small- x

electron-proton scattering. The only additional requirement is for forward neutron detectors with specifications similar to that for the ZEUS forward neutron calorimeter (FNC). These will be needed to trigger on central inelastic collisions by selecting events where a larger than average number of neutrons is produced. Note that for small x collisions at central impact parameters the virtual photon interacts inelastically with $\sim A^{1/3}$ nucleons. On the basis of an analysis [68] of E-665 data on the production of soft neutrons at $x \sim 0.03$ [70], we estimate that the average number of soft neutrons produced in the central collisions will be ~ 20 (as compared to ~ 4 for peripheral inelastic collisions). Overall, a strong correlation between the number produced nucleons and centrality of the event is expected at small x (as is also the case for hadron-nucleus scattering). As we explained above, such detectors would allow the breakdown of leading twist QCD to be studied in runs with a single heavy nucleus.

A FNC-type neutron calorimeter would have nearly 100% acceptance for the neutrons from nuclear break-up. Since the average number of such neutrons exceeds one for $A \geq 16$, a FNC-type detector would allow an effective tagging of nuclear break-up. Hence, it would also simplify studies of diffractive processes with nuclei. The separation of the three classes of diffractive events (coherent scattering, nuclear break-up producing nuclear fragments (mostly neutrons and protons) in the forward direction, and diffractive dissociation with meson production in the nucleus fragmentation region from non-diffractive reactions) is very similar to the selection of diffractive events in the ep case (see the previous subsection). The contribution of diffractive dissociation to the overall diffractive cross section is significantly smaller than in the ep case. The experimental signatures for this class of reactions are similar to ep scattering since the energy flow in the forward direction is expected to have almost the same topology. Calorimetric coverage down to $\theta \leq 1^\circ$ in the forward region will allow for the detection of most dissociative reactions. Nuclear break-up is expected to constitute about 10% of coherent diffraction for a wide range of model parameters (see Fig. 10). In the case of coherent exclusive processes, such as coherent vector meson production, detection of the process will be further simplified since the average transverse momenta of coherently

produced vector mesons are $p_t \leq 2/R_A^2$, which is much smaller than for exclusive processes with protons.

VII. CONCLUSIONS

The nuclear program at THERA has a very strong potential for the discovery of a number of interesting new high energy (small x) phenomena, including quark and gluon shadowing (for kinematics in which longitudinal distances are much larger than the heavy nuclear radius), hard coherent diffraction off nuclei and colour opacity in the production and interaction of small colour singlets. Crucially, for the first time, it will provide several effective tools for unambiguously probing the black body limit of photon-nuclear collisions, thereby investigating QCD in a new regime of strong interactions with a small coupling constant.

We thank A. H. Mueller for a useful discussion and GIF, ARC, PPARC and DOE for support. LF and MS thank INT for hospitality during the time this work was completed.

FIGURES

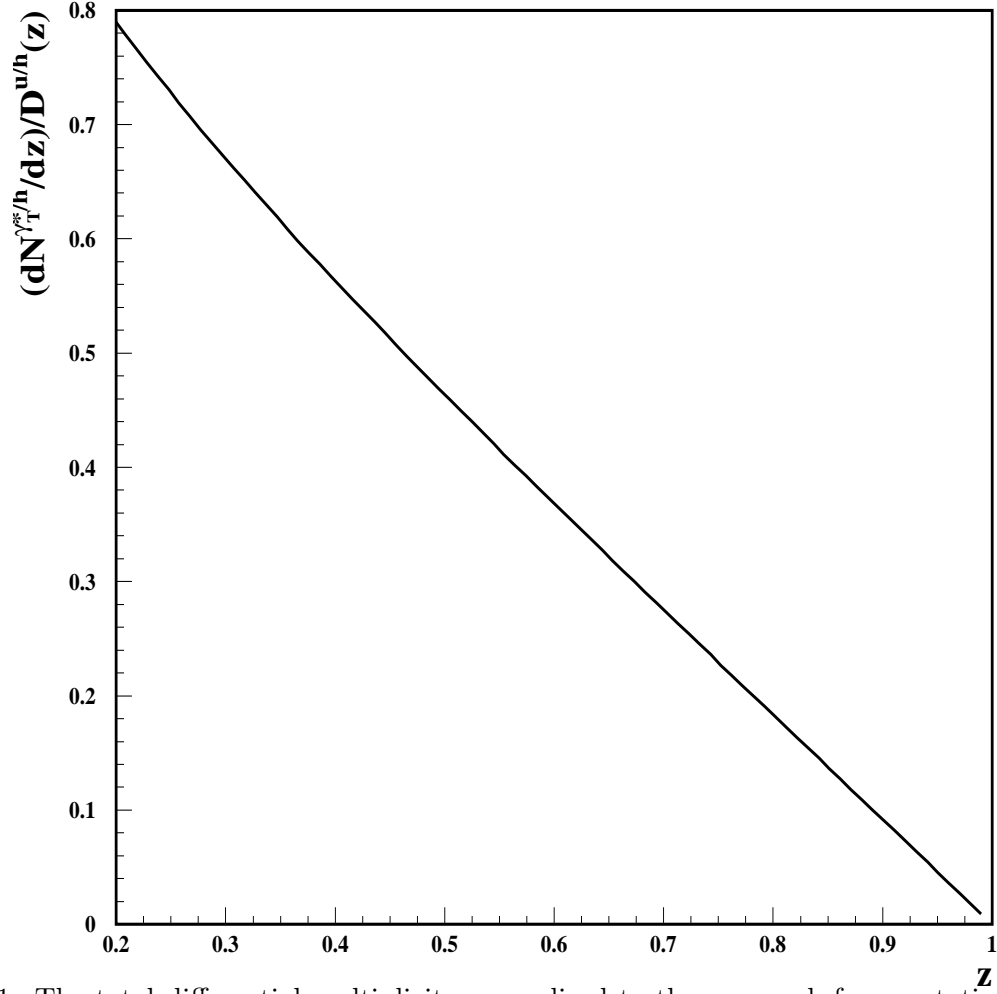


FIG. 1. The total differential multiplicity normalized to the up quark fragmentation function [45], $(dN_T^{*h}/dz)/D^{u/h}(z, Q^2)$, as a function of z at $Q^2=2 \text{ GeV}^2$ calculated in the BBL using (25).

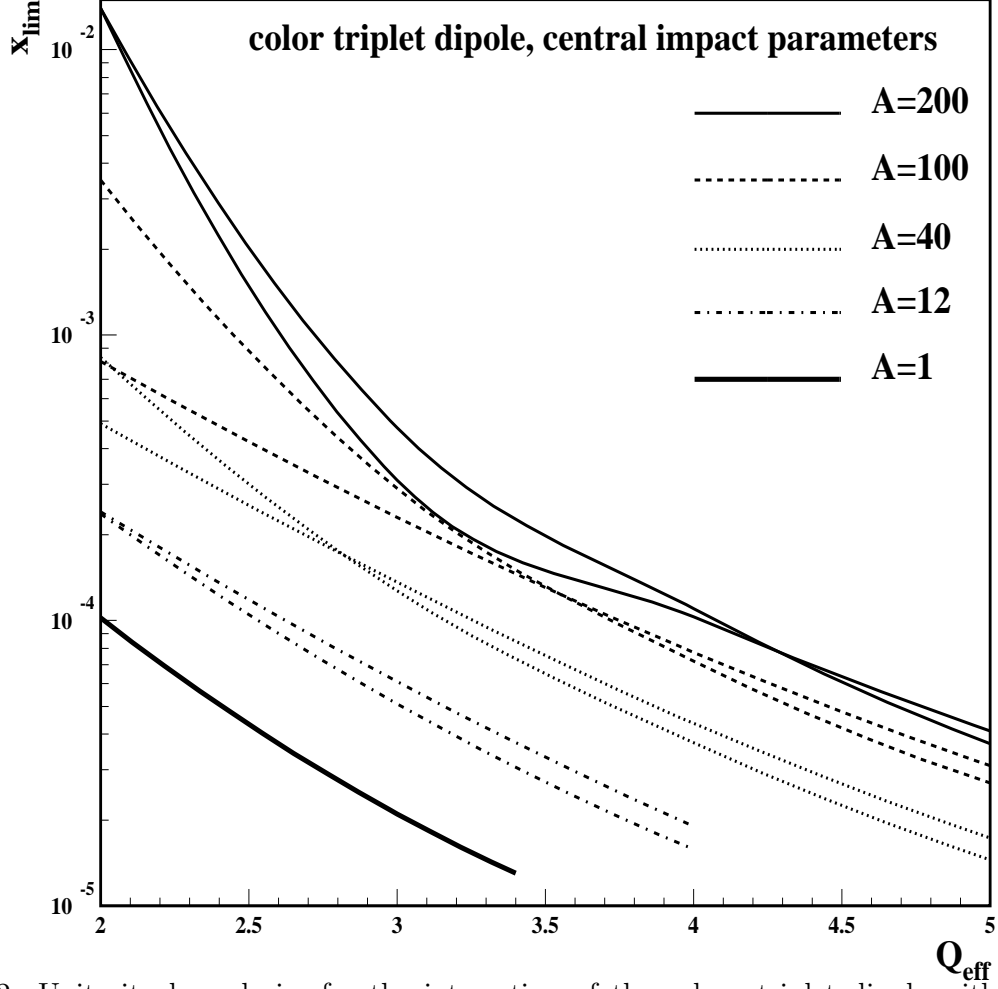


FIG. 2. Unitarity boundaries for the interaction of the colour triplet dipole with nuclei at central impact parameters. Regions to the left of each curve are prohibited by the unitarity bound of (31). Two sets of curves are given for each nucleus correspond to two different models of leading twist shadowing (as discussed in subsection V).

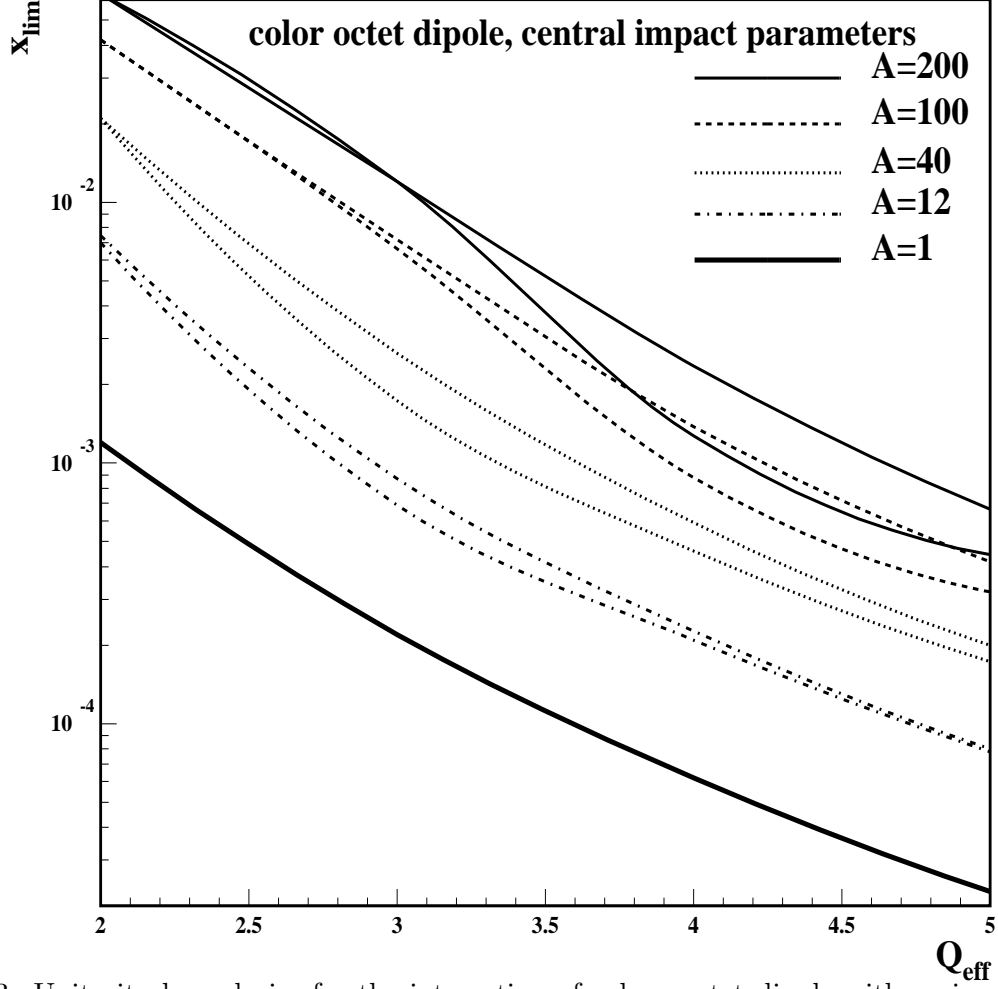


FIG. 3. Unitarity boundaries for the interaction of colour octet dipole with various nuclei at central impact parameters. Regions to the left of each curve are prohibited by the unitarity bound of (32). Two sets of curves are given for each nucleus correspond to two different models of leading twist shadowing (as discussed in subsection V).

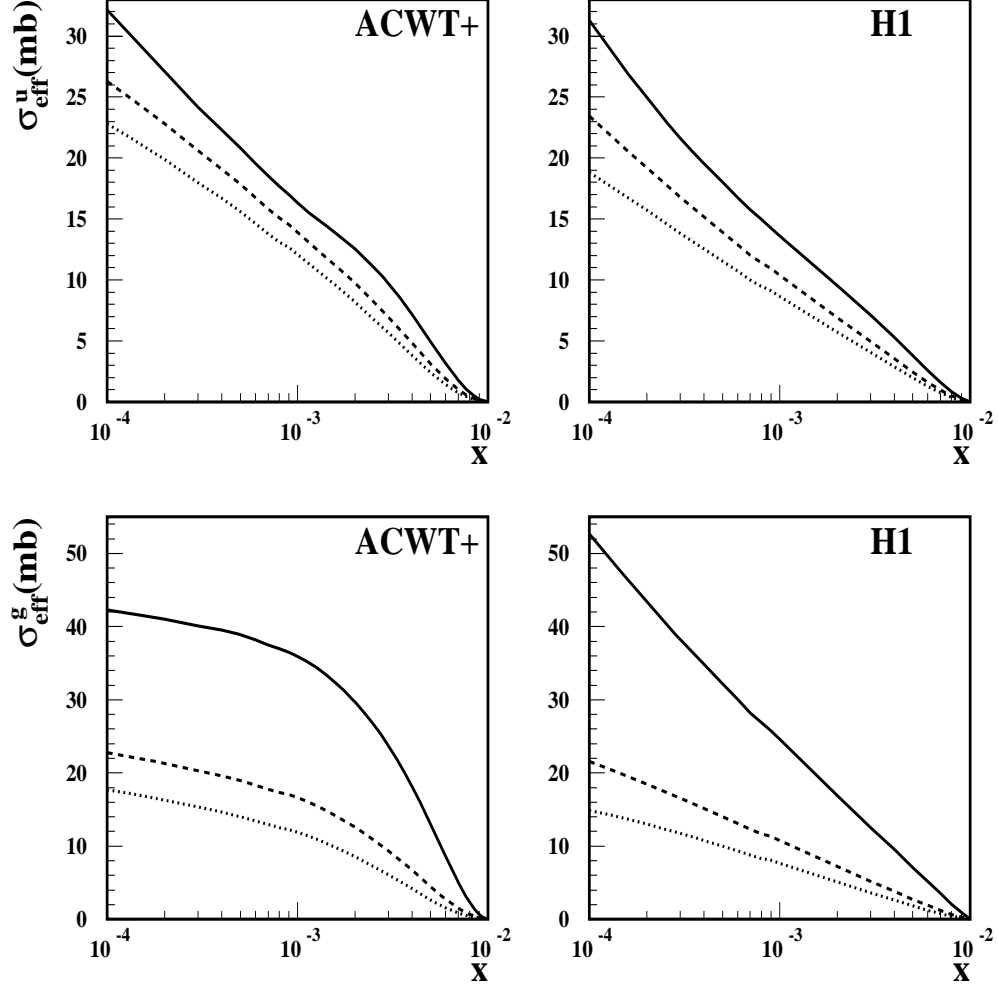


FIG. 4. The effective cross section for nuclear shadowing (or nucleon diffraction) of (34), σ_{eff}^j , for a parton of type $j = u, g$, as a function of Bjorken x at several values of Q^2 . The solid curve is for $Q = 2$ GeV, the dashed curve is for $Q = 5$ GeV, the dotted one is for $Q = 10$ GeV. Two representative [63] sets of diffractive parton distributions have been used in the curves labelled by “ACWT+” [62] and “H1” [58] (see text).

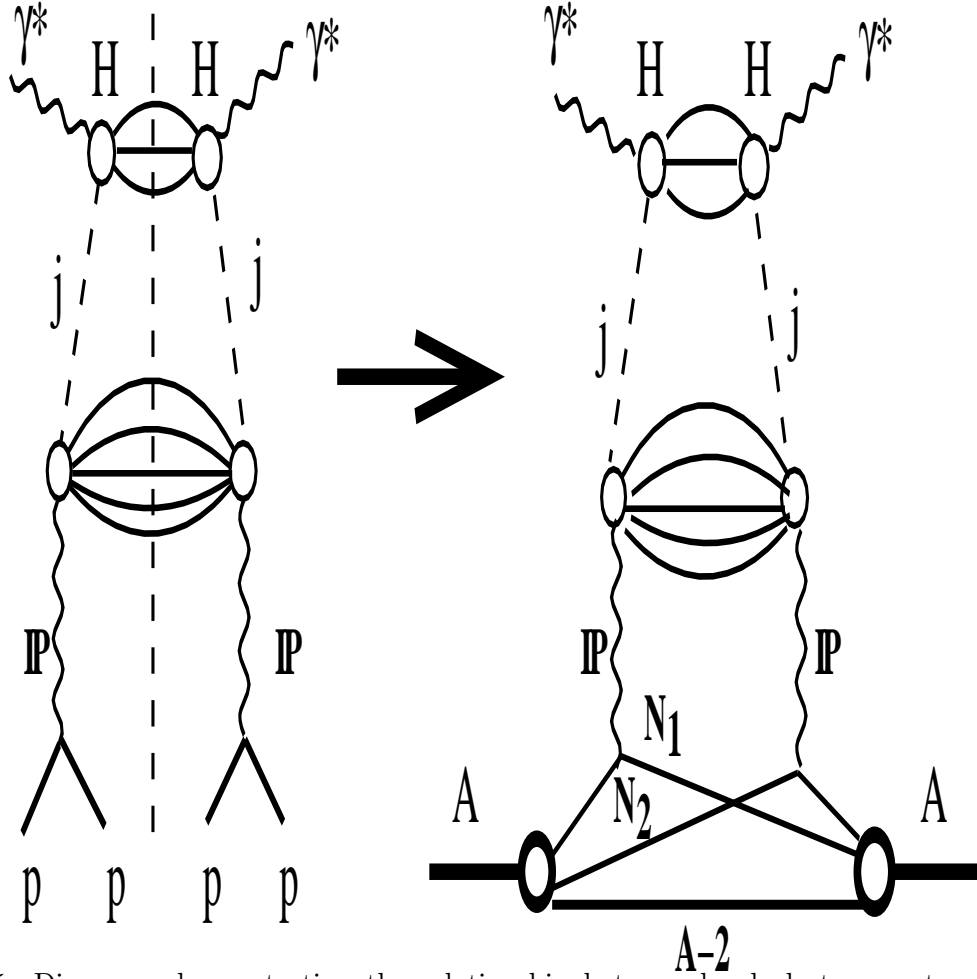


FIG. 5. Diagrams demonstrating the relationship between hard electron-proton diffraction, involving a parton of type j , and nuclear shadowing in inclusive DIS. Here the Pomeron symbol, P , merely represents a generic label for vacuum exchange.

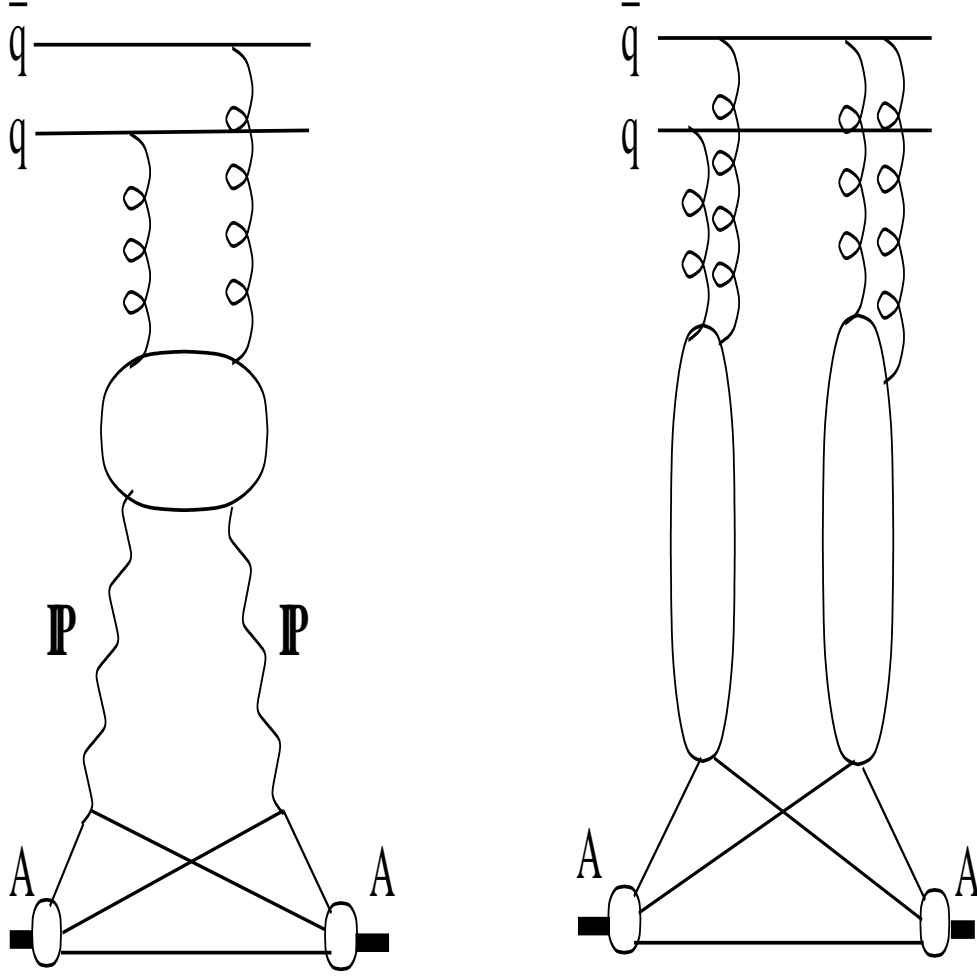


FIG. 6. Typical diagrams for the leading twist (left) and eikonal (right) models for nuclear shadowing involving a small dipole and two nucleons. The curly lines represent gluons. In the diagram on the right the blob and its attached legs represent the gluon distribution of the nucleon. The Pomeron symbol, \mathbb{P} , in the diagram on the left merely represents a generic label for vacuum exchange.

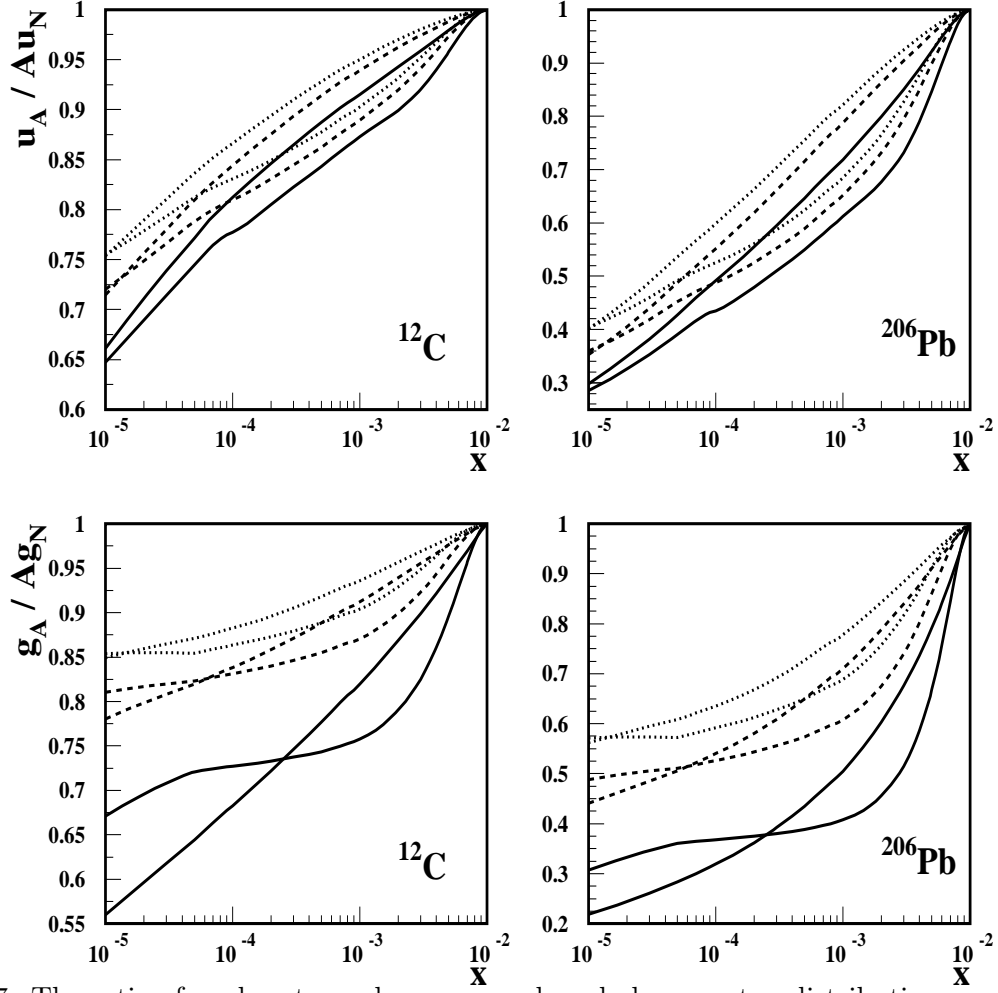


FIG. 7. The ratio of nuclear to nucleon up-quark and gluon parton distributions as a function of x , scaled by nucleon number, A . Two representative [63] sets of diffractive parton densities, “ACWT+” [62] and “H1” [58], are used to calculate nuclear shadowing (see text) for each nucleon and taken together they give an indication of the spread of theoretical predictions. The solid, dashed, and dotted curves are for $Q = 2, 5, 10$ GeV, respectively.

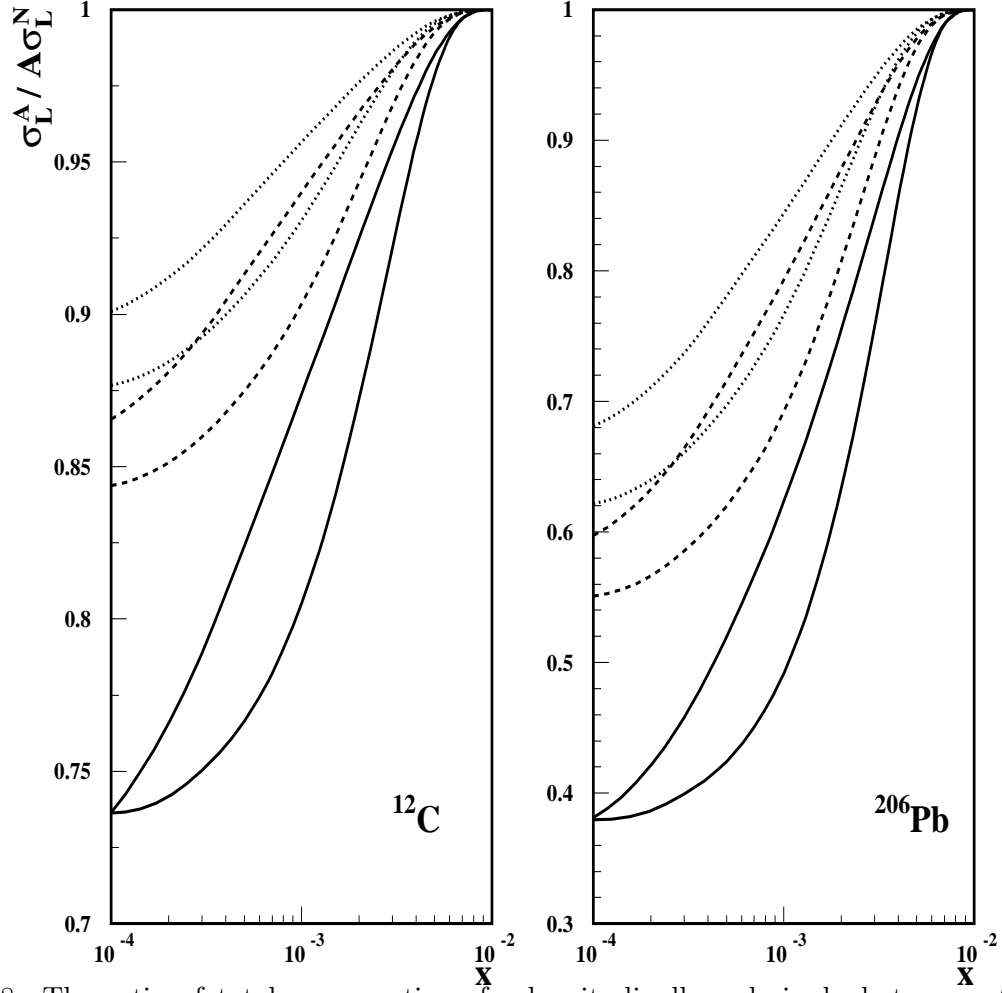


FIG. 8. The ratio of total cross sections for longitudinally polarised photons scattering on nuclear and nucleon targets, $\sigma_L^A / (A\sigma_L^N)$, as function of x for Carbon and Lead. Two representative [63] sets of diffractive parton densities are used, “ACWT+” [62] and “H1” [58], to calculate nuclear shadowing. The solid, dashed and dotted curves are for $Q = 2, 5, 10$ GeV, respectively.

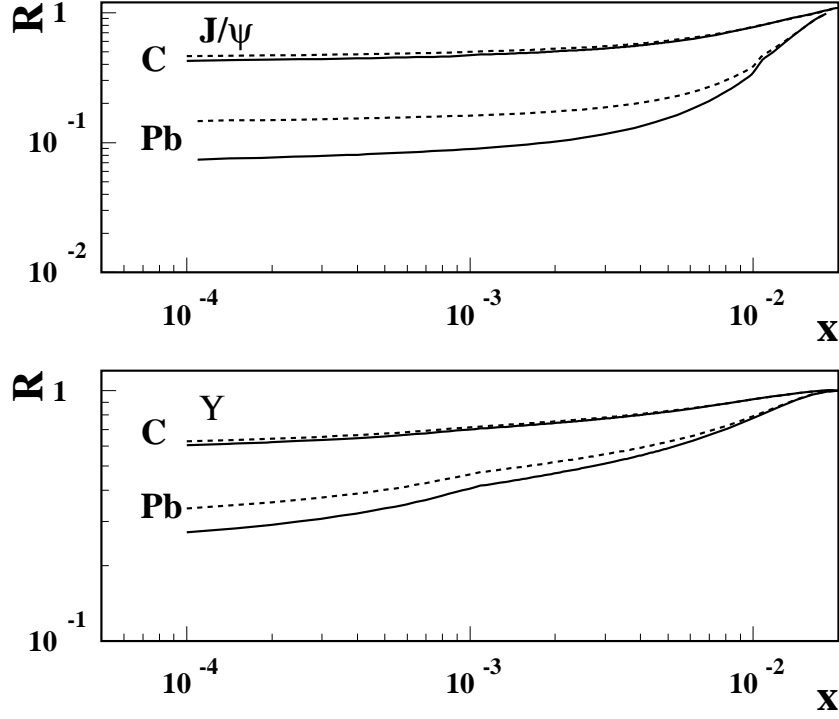


FIG. 9. The colour opacity effect for the ratio, R , of the coherent production of J/ψ and Υ from Carbon and Lead, normalized to the value of this ratio at $x = 0.02$, calculated in the leading twist models of gluon shadowing [65] both with (dashed curves) and without (solid curves) taking the fluctuations of the cross section into account.

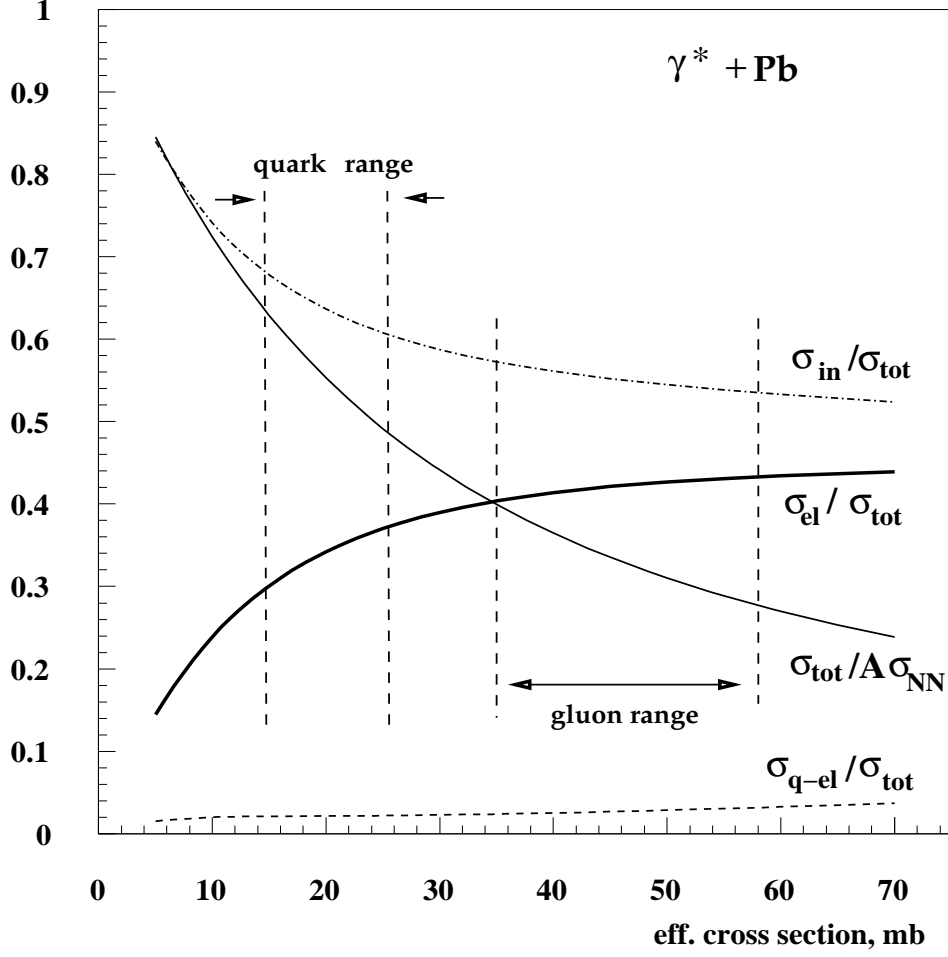


FIG. 10. Fractions of the total cross section, given by inelastic scattering (*in*), coherent (*el*) and incoherent (*q-el*) diffractive scattering cross sections as a function of the average interaction strength for quarks and gluons (σ_{eff}^j of (34), cf. Fig. 4) for scattering off Lead.

REFERENCES

- [1] V.N. Gribov and L.N. Lipatov, Sov. J. Phys. **15** (1972) 438,625;
Yu.L. Dokshitzer, JETP **46** (1977) 641;
G. Altarelli and G. Parisi, Nucl. Phys. **B126** (1977) 298.
- [2] J.C. Collins, D.E. Soper, and G. Sterman, Nucl. Phys. **B 308** (1988) 833.
- [3] H. Georgi and H.D. Politzer, Phys. Rev. **D9** (1974) 416;
D. Gross and F. Wilczek, Phys. Rev. **D9** (1974) 980.
- [4] J.D. Bjorken, Phys. Rev. **179** (1969) 1547.
- [5] M. Glück, E. Reya and A. Vogt, Eur. Phys. J. **C5** (1998) 461;
A.D. Martin et al., Eur. Phys. J. **C4** (1998) 463;
CTEQ Coll., H. Lai et al., Eur. Phys. J. **C12** (2000) 375.
- [6] J.C. Collins, Phys. Rev. D **57**, 3051 (1998).
- [7] S. J. Brodsky et al., Phys. Rev. **D50** (1994) 3134.
- [8] J.C. Collins, L. Frankfurt and M. Strikman, Phys. Rev. **D56**, 2982 (1997).
- [9] J.C. Collins and A. Freund, Phys. Rev. **D59**, 074009 (1999).
- [10] H. Abramowicz and A. Caldwell, Rev. Mod. Phys. **71**, 1275 (1999).
- [11] L. Frankfurt, V. Guzey and M. Strikman, J. Phys. **G 27** (2001) R23.
- [12] M. Wüsthoff and A.D. Martin, J. Phys. **G25**, R309 (1999).
- [13] A. Hebecker, Phys. Rept. **331**, 1 (2000).
- [14] L. Frankfurt, G. A. Miller and M. Strikman, Phys. Lett. **B304** (1993) 1;
B. Blattel et al., Phys. Rev. Lett. **71** (1993) 896.
- [15] E791 Coll., E.M. Aitala et al., *Observation of color-transparency in diffractive dissociation of pions*, [hep-ex/0010044];

Direct measurement of the pion valence quark momentum distribution, the pion light-cone wave function squared, [hep-ex/0010043].

- [16] M. Sokoloff et al., Phys. Rev. Lett. **57** (1986) 3003.
- [17] L. Frankfurt and M. Strikman, Phys. Rev. Lett. **63** (1989) 1914, Erratum-ibid. **64** (1990), 815.
- [18] L.L. Frankfurt, W. Koepf and M. Strikman, Phys. Rev. **D54** (1996) 3194.
- [19] L.L. Frankfurt, W. Koepf and M. Strikman, Phys. Rev. **D57** (1998) 512.
- [20] M.G. Ryskin, Z. Physik **57** (1993) 89.
- [21] A.D. Martin, M.G. Ryskin and T. Teubner, Phys. Rev. **D55** (1997) 4329; Phys. Rev. **D56** (1997) 3007; Phys. Rev. **D62** (2000) 014022.
- [22] L.L. Frankfurt, M.M. McDermott and M. Strikman, JHEP **02** (1999) 002; *A fresh look at diffractive J/ψ photoproduction at HERA, with predictions for THERA*, [hep-ph/0009086].
- [23] A.D. Martin, M.G. Ryskin and T. Teubner, Phys Lett. **B454** (1999) 339.
- [24] L. Frankfurt, A. Freund and M. Strikman, Phys. Rev. **D58** (1998) 114001, Erratum-ibid. **D59** (1999) 119901; Phys. Lett. **B460** (1999) 417.
- [25] H. Abramowicz, L.L. Frankfurt, and M. Strikman, DESY 95-047, March 1995; Proceedings of SLAC Summer Inst., 1994, pp. 539-574; Surveys High Energ. Phys. **11**, 51 (1997).
- [26] H1 Coll., S. Aid et al., Nucl. Phys. **B 470** (1996) 3.
- [27] ZEUS Coll., M. Derrick et al., Z. Phys. **C 72** (1996) 399.
- [28] V.S. Fadin, E.A. Kuraev and L.N. Lipatov, Phys. Lett. **B60**, 50 (1975); Sov. Phys. JETP **45**, 199 (1977);

- I.I. Balitsky and L.N. Lipatov, Sov. J. Nucl. Phys. **28**, 822 (1978); V.S. Fadin and L.N. Lipatov, Phys. Lett. B **429**, 127 (1998).
- [29] G. Camici and M. Ciafaloni, Phys. Lett. B **412**, 396 (1997).
- [30] J.R. Forshaw and D.A. Ross, *Quantum Chromodynamics and the Pomeron*, (Cambridge Univ. Press (1997) 248p).
- [31] M. McDermott et al., Eur. Phys. J. C **16**, 641 (2000).
- [32] L. Frankfurt, A. Radyushkin and M. Strikman, Phys. Rev. **D55** (1997) 98.
- [33] F.E. Low, Phys. Rev. **D12** (1975) 163.
- [34] M. Froissart, Phys. Rev. **123** (1961) 1053.
- [35] A.H. Mueller and J. Qiu, Nucl. Phys. **B268**, 427 (1986).
- [36] A. De Rejula et al., Phys. Rev. **D10** (1974) 1649.
- [37] R.J Eden et al., *The Analytic S-matrix*, (Cambridge Univ. Press (1966), 287p).
- [38] A.H. Mueller, Nucl. Phys. B **335**, 115 (1990); Nucl. Phys. **B558** (1999) 285.
- [39] V.N.Gribov, Zh. Eksp. Teor. Fiz. **57** (1969) 1306.
- [40] J.D. Bjorken and J.B. Kogut, Phys. Rev. **D8** (1973) 1341.
- [41] R.K. Ellis, W.J. Stirling and B.R. Webber, *QCD and collider physics*, (Cambridge Univ. Press (1996) 435p, Cambridge Monographs on Particle Physics, Nuclear Physics and Cosmology, Vol. 8).
- [42] J.J. Sakurai, Phys. Rev. Lett. **22**, 981 (1969).
- [43] L. Frankfurt, V. Guzey and M. Strikman, Phys. Rev. **D 58** (1998) 094039.
- [44] H. Fraas, B.J. Read and D. Schildknecht, Nucl. Phys. **B86** (1975) 346;
G. Cvetič, D. Schildknecht and A. Shoshi, Acta Phys. Polon. **B30** (1999) 3265;

- A. Donnachie and G. Shaw, in: *Electromagnetic interactions of hadrons, Vol.2*, 169, eds. A. Donnachie and G. Shaw (Plenum, New York (1978));
- G. Shaw, Phys. Rev. **D47** (1993) R3676;
- G. Shaw, Phys. Lett. **B228** (1989) 125;
- P. Ditsas and G. Shaw, Nucl. Phys. **113** (1976) 246.
- [45] L. Bourhis et al., *Next-to-leading order determination of fragmentation functions*, [hep-ph/0009101].
- [46] J. Jalilian-Marian et al., Phys.Rev. **D59** (1999) 034007; Erratum-ibid. **D59** (1999) 099903 and references therein; L. McLerran and R. Venugopalan, Phys. Rev. **D49** (1994) 2233.
- [47] European Muon Coll., J. Ashman et al. Z. Phys. C **52**, 1 (1991).
- [48] W. Buchmueller, A. Hebecker and M.F. McDermott, Nucl. Phys. **B487** (1997) 283, Erratum ibid. **B500** (1997) 621.
- [49] L. Frankfurt, M. Strikman and S. Liuti, *Parton Distributions In Hard Nuclear Collisions*, in “Brookhaven 1990, Experiments and detectors for a relativistic heavy ion collider”, 103.
- [50] H.L. Lai et al., Phys. Rev. **D55** (1996) 1280.
- [51] V.N. Gribov, Zh. Exp. Teor. Fiz. **57** 1309 (1969); Sov. Phys. JETP **30** (1970) 709.
- [52] L. Frankfurt and M. Strikman, Phys.Lett. **B382** (1996) 6.
- [53] L. McLerran and R. Venugopalan, Phys.Rev. **D50** (1994) 225.
- [54] L.L. Frankfurt and M.I. Strikman, Phys. Rept. **160** (1988) 235.
- [55] L.L. Frankfurt and M.I. Strikman, Nucl. Phys. **B316** (1989) 340.
- [56] New Muon Coll., P. Amaudruz et al., Nucl. Phys. B **441** (1995) 3.

- [57] A. Capella et al., Eur. Phys. J. **C5** (1998) 111.
- [58] H1 Coll., C. Adloff et al., Z. Phys. C **76** (1997) 613.
- [59] ZEUS Coll., J. Breitweg et al., Eur. Phys. J. **C6** (1999) 43.
- [60] J.C. Collins, Phys. Rev. **D57** (1998) 3051.
- [61] E. Feinberg and Ya. Pomeranchuk, Suppl. Nuovo Cimento **111** (1956) 652; M. Good and W. Walker, Phys. Rev. **D120** (1960) 1857.
- [62] L. Alvero, et al. Phys. Rev. **D59** (1999) 074022.
- [63] F. Hautmann, Z. Kunszt and D.E. Soper, Nucl. Phys. **B563** (1999) 153.
- [64] L. Frankfurt, V. Guzey, M. McDermott, M. Strikman, in preparation.
- [65] L. Frankfurt and M. Strikman, Eur. Phys. J. **A5** (1999) 293.
- [66] L. Alvero, L.L. Frankfurt and M.I. Strikman, Eur. Phys. J. **A5** (1999) 97.
- [67] V. Abramovskii, V.N. Gribov, and O.V. Kancheli, Sov. J. Nucl. Phys. **18** (1974) 308.
- [68] M. Strikman, M.G. Tverskoi and M.B. Zhalov, Phys. Lett. **B459** (1999) 37.
- [69] M. Arneodo et al., *Nuclear beams in HERA*, in “Hamburg 1995/96, Future physics at HERA”, 887, [hep-ph/9610423].
- [70] E665 Coll., M.R. Adams et al., Phys. Rev. Lett. **74** (1995) 5198.